7-2018

Impacts of Atmospheric Nitrogen Deposition and Coastal Nitrogen Fluxes on Oxygen Concentrations in Chesapeake Bay

Fei Da
Virginia Institute of Marine Science

Marjorie A.M. Friedrichs
Virginia Institute of Marine Science, marjy@vims.edu

Pierre St-Laurent
Virginia Institute of Marine Science, pst-laurent@vims.edu

Journal of Geophysical Research: Oceans

RESEARCH ARTICLE
10.1029/2018JC014009

Key Points:
- Atmospheric dissolved inorganic nitrogen deposition has about the same gram for gram impact on Chesapeake Bay hypoxia as riverine loading
- Atmospheric nitrogen deposition and shelf nitrogen concentrations have their greatest impact on Chesapeake Bay hypoxia during the summer
- The greatest impacts of atmospheric deposition and shelf nitrogen concentrations are farther downstream in wet years compared to dry years

Supporting Information:
- Supporting Information S1

Correspondence to:
F. Da,
fda@vims.edu

Citation:
Da, F., Friedrichs, M. A. M., & St-Laurent, P. (2018). Impacts of atmospheric nitrogen deposition and coastal nitrogen fluxes on oxygen concentrations in Chesapeake Bay. *Journal of Geophysical Research: Oceans*, *123*, 5004–5025. https://doi.org/10.1029/2018JC014009

Received 24 MAR 2018
Accepted 22 JUN 2018
Accepted article online 2 JUL 2018
Published online 28 JUL 2018

Impacts of Atmospheric Nitrogen Deposition and Coastal Nitrogen Fluxes on Oxygen Concentrations in Chesapeake Bay

Fei Da[1], **Marjorie A. M. Friedrichs**[1], **and Pierre St-Laurent**[1]

[1]Virginia Institute of Marine Science, College of William & Mary, Gloucester Point, VA, USA

Abstract Although rivers are the primary source of dissolved inorganic nitrogen (DIN) inputs to the Chesapeake Bay, direct atmospheric DIN deposition and coastal DIN concentrations on the continental shelf can also significantly influence hypoxia; however, the relative impact of these additional sources of DIN on Chesapeake Bay hypoxia has not previously been quantified. In this study, the estuarine-carbon-biogeochemistry model embedded in the Regional-Ocean-Modeling-System (*Ches*ROMS-ECB) is used to examine the relative impact of these three DIN sources. Model simulations highlight that DIN from the atmosphere has roughly the same impact on hypoxia as the same gram-for-gram change in riverine DIN loading, although their spatial and temporal distributions are distinct. DIN concentrations on the continental shelf have a similar overall impact on hypoxia as DIN from the atmosphere (~0.2 mg L^{-1}); however, atmospheric DIN impacts dissolved oxygen (DO) primarily via the decomposition of autochthonous organic matter, whereas coastal DIN concentrations primarily impact DO via the decomposition of allochthonous organic matter entering the Bay mouth from the shelf. The impacts of atmospheric DIN deposition and coastal DIN concentrations on hypoxia are greatest in summer and occur farther downstream (southern mesohaline) in wet years than in dry years (northern mesohaline). Integrated analyses of the relative contributions of all three DIN sources on summer bottom DO indicate that impacts of atmospheric deposition are largest in the eastern mesohaline shoals, riverine DIN has dominant impacts in the largest tributaries and the oligohaline Bay, while coastal DIN concentrations are most influential in the polyhaline region.

Plain Language Summary Most organisms living in the Chesapeake Bay, like fish, crabs, and oysters, need adequate oxygen concentrations to survive. However, general increases in the supply of nutrients to estuaries always enhance the production of algae, and the decomposition of these algae takes away oxygen from other organisms, resulting in hypoxic (low-oxygen) conditions or what is commonly referred to as a "dead zone." Generally, researchers focus on how terrestrial nutrients entering the bay, for example, from fertilizer, wastewater treatment, or sewer runoff, produce the Chesapeake Bay dead zone, since they account for most of the nutrients entering the bay. However, the atmospheric and oceanic nutrients directly impacting the bay are often not accurately considered. In this study the impacts of nutrients from the atmosphere and the open ocean on Chesapeake Bay hypoxia are quantified via the application of a three-dimensional ecosystem model. Atmospheric deposition of nitrate is found to have the same gram-for-gram impact on hypoxia as terrestrial nitrate entering via rivers. Overall, these two sources of nutrients have the greatest impact in the summer and have similar impacts on dissolved oxygen, reducing oxygen concentrations by up to 0.2 mg L^{-1} in the mid-Chesapeake Bay region where oxygen concentrations are lowest.

1. Introduction

The Chesapeake Bay (Figure 1) is the largest and most productive estuary in the continental United States and plays a crucial role in coastal nitrogen transformations, transport, and burial (Bronk et al., 1998; Kemp et al., 2005); however, this estuary has been continually impacted by human activities ever since Europeans migrated to the region four centuries ago. Urbanization, industrial expansion, and fertilizer usage are major factors contributing to the rapid increase of dissolved inorganic nitrogen (DIN) loads and concentrations in the Chesapeake Bay prior to the mid-1980s, which led to algal blooms and severe eutrophication (Nixon, 1995). One of the most serious issues caused by eutrophication and the resulting algal blooms is hypoxia, which is typically defined as dissolved oxygen concentration (DO) less than 2 mg L^{-1} (Seliger et al., 1985). In the Chesapeake Bay, hypoxia was first observed in the 1930s (Newcombe & Horne, 1938). Since the rapid increase of DIN loadings in the 1960s and 1970s, hypoxia has been observed every year in the Bay (Bever

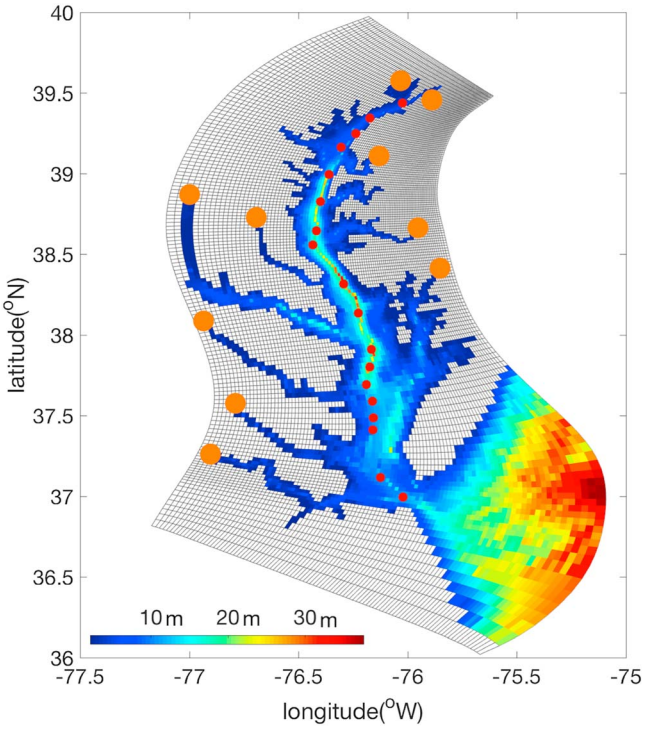

Figure 1. The Chesapeake Bay bathymetry, horizontal coordinate system (light gray grid cells) of *Ches*ROMS-ECB and stations (red dots) along the mainstream of the bay (stations from oligohaline to polyhaline bay are as follows: CB2.1, CB2.2, CB3.1, CB3.2, CB3.3C, CB4.1C, CB4.2C, CB4.3C, CB5.1, CB5.2, CB5.3, CB5.4, CB5.5, CB6.1, CB6.2, CB6.3, CB7.3, and CB7.4). The orange circles denote the 10 locations of watershed inputs, representing the locations of the largest rivers entering the bay.

et al., 2013; Hagy et al., 2004). During the summer, the accelerating rate of microbial decomposition of organic matter increases oxygen consumption in both the water column and the sediments. Together with strengthened vertical stratification and reduced solubility, DO concentrations decrease, eventually resulting in hypoxia or even anoxia (DO < 0.2 mg L^{-1}) in deep bottom waters (Murphy et al., 2011). A study on Chesapeake Bay hypoxia using 3-D numerical models indicated that the volume of hypoxic water in the Bay ranged between 8 and 17 km^3 from 1985 to 2011 (Bever et al., 2013). Within this large volume of low oxygen water, benthic macrofauna struggle with hypoxic stress (Diaz & Rosenberg, 1995), and hypoxia-related diseases (Holland et al., 1987). For example, the abundance of benthic macrofauna is typically low in hypoxic water, and sulfide accumulation in anoxic water is toxic to them.

Over the past three decades, many management actions have been taken to try to reduce DIN inputs to the bay from the watershed in order to reduce the harmful impacts of hypoxia. Due to the large land to water ratio (14:1), riverine DIN accounts for most of the DIN input to the Chesapeake Bay, and thus, seasonal and long-term variability of water quality is highly sensitive to the amount of freshwater flow (Hagy et al., 2004; Kemp et al., 2005). Between World War II and the late 1980s, the nitrate (NO_3^-) loading in the Susquehanna River increased by almost a factor two (Harding et al., 2016). Because of recent management efforts (e.g., the establishment of the Chesapeake Bay total maximum daily load), flow-adjusted NO_3^- loadings have been reduced by 5.4% since 1981 (Harding et al., 2016). However, projected climate change may be counter acting the impact these riverine nutrient reductions are having on Chesapeake Bay hypoxia (Irby et al., 2018).

Atmospheric deposition is another important source of DIN for coastal waters of the U.S. east coast (Paerl et al., 1999, 2002; St-Laurent et al., 2017). In the Chesapeake Bay, nearly half of the total atmospheric DIN deposition stems from emission sources outside of the Bay watershed (USEPA, 2010a). Nitrate deposition is primarily from combustion of fossil fuels by industries and automobiles (Russell et al., 1998), while agricultural usage of fertilizers, farmed animal excreta, and biomass burning are primary contributors to anthropogenic ammonium (NH_4^+) deposition (Prospero et al., 1996). Early studies indicated that total atmospheric nitrogen deposition, including both the "direct" component falling on Chesapeake Bay waters and the "indirect" component falling on land and being washed into the Bay, accounted for up to 40% of the total anthropogenic nitrogen loadings to the Chesapeake Bay during the mid-1980s (Fisher & Oppenheimer, 1991; Hinga et al., 1991). Encouragingly, the largest component of atmospheric DIN deposition, that is, NO_3^-, has decreased up to 30% since 1985 due to the Clean Air Act, albeit with some interannual variability. In contrast, large increases in NH_4^+ wet deposition (~40–50%) have been observed in Maryland and North Carolina since 1985 (Y. Li et al., 2016). By the early 21st century, direct atmospheric deposition of DIN was reduced to roughly 10–15% of the total DIN inputs to the Chesapeake Bay (Linker et al., 2013).

Continental shelf waters with high DIN concentrations can be another potential source of nutrients to estuaries. In the Pacific Northwest, coastal upwelling provides a significant source of DIN to shallow shelf and estuarine waters (Brown & Ozretich, 2009; Davis et al., 2014; Hickey & Banas, 2003). However, studies estimating DIN inputs from the continental shelf to the Chesapeake Bay are quite limited. Northeast winds during the summer could be upwelling favorable in the Middle Atlantic Bight (Blanton et al., 1985; Pietrafesa et al., 1994), bringing relatively high DIN concentration subsurface shelf water to the adjacent region (Janowitz & Pietrafesa, 1982; Pietrafesa et al., 1994). Cross-isobath fluxes of nutrient-rich waters (e.g., Labrador current) and winter mixing replenish the surface nutrient concentrations in the Middle Atlantic Bight (Townsend et al., 2006). Williams et al. (2011) estimated that NO_3^- concentrations in the Middle Atlantic Bight were less than 0.14 mg L^{-1} in depths $<$300 m and were greater than 0.29 mg L^{-1} in denser waters at depths of 300–500 m, both of which are much higher than NO_3^- concentrations ($<$0.01 mg L^{-1}) in surface waters near the

mouth of the Chesapeake Bay. Although previous studies indicate that the Chesapeake Bay is likely a net source of DIN to the continental shelf over long (interannual) time scales (Feng et al., 2015; Jiang & Xia, 2018; Kemp et al., 1997), at certain times of the year, DIN in continental shelf waters enters the Bay at depth via estuarine circulation, potentially impacting DO concentrations and primary production (PP) in the bay.

In this study, a numerical model is used to better understand and quantify the relative magnitude of the impacts these three different sources of DIN have on PP and hypoxia in Chesapeake Bay. By including all three sources of DIN (atmospheric, terrestrial, and coastal ocean), a more realistic simulation of biogeochemical dynamics is generated for the Chesapeake Bay. In section 2 the data and models used in this study are described. Results of a 4-year hindcast from 2002 to 2005 are presented in section 3, along with the results of six sensitivity experiments in which each of the three different sources of DIN is increased/decreased independently in order to estimate their relative importance on PP and DO. Seasonal, interannual, and spatial differences in these impacts are discussed in section 4, and the findings are summarized in section 5.

2. Methods

2.1. CBP Available Data

A plethora of in situ data is available for model evaluation in the Chesapeake Bay. Most notably, the Chesapeake Bay Program (CBP) has been thoroughly monitoring Chesapeake Bay water quality since 1984. Available CBP biogeochemical data, generally measured once each month from October to March, and twice each month from April to September, include concentrations of DIN (here defined as the sum of NO_3^- and NH_4^+), DO, dissolved organic nitrogen (DON), particulate organic nitrogen (PON), chlorophyll, total suspended solids, and surface diffuse attenuation of light (K_D). Vertical profiles of DO are measured at approximately 1-m intervals throughout the water column; other variables are sampled at the surface and bottom and at middle level depths as well. In this study, model-data comparisons (see Online Supporting Information) are focused on 18 main stem stations (Figure 1).

2.2. *Ches*ROMS-ECB Model Description

A three-dimensional hydrodynamic-biogeochemistry model, *Ches*ROMS-ECB, is used to address research questions pertaining to the impact of nitrogen inputs from the atmosphere and shelf. *Ches*ROMS-ECB is an estuarine-carbon-biogeochemistry (ECB) model embedded in the three-dimensional regional ocean modeling system (ROMS; Feng et al., 2015; Irby et al., 2016, 2018) and uses the *Ches*ROMS grid of Xu et al. (2012).

Physical components of the model are from ROMS version 3.6 (Shchepetkin & McWilliams, 2005), which is a free-surface, terrain-following, primitive equation ocean model. Vertically, governing equations are discretized over a stretched terrain-following coordinates with 20 levels (Shchepetkin & McWilliams, 2005). The horizontal grid has orthogonal curvilinear coordinates with highest resolution (430 m) in the northern Bay and lowest resolution (~10 km) at the open boundary in the southern end of Middle Atlantic Bight (Figure 1). The Multidimensional Positive Definite Advection Transport Algorithm is applied to guarantee all variables at each time step are positive definite (Smolarkiewicz, 1983, 1984). The model was forced at the open boundary by tidal constituents from the Advanced Circulation model and by observed nontidal water levels from Duck, NC and Lewes, DE (Scully, 2016). Temperature, salinity, and DO were nudged to the World Ocean Atlas monthly climatological data along the open boundary. Atmospheric forcing (e.g., 10-m winds, short-wave radiation, rainfall, surface air humidity, air temperature, and pressure) was derived from the North American Regional Reanalysis (Mesinger et al., 2006).

Although the ECB ecosystem module includes both nitrogen and carbon cycles, the work described here only involves the nitrogen component. This includes 11 state variables: NO_3^-, NH_4^+, phytoplankton, zooplankton, small and large detritus, semilabile and refractory DON, inorganic suspended solids (ISSs), DO, and chlorophyll (Feng et al., 2015). At the bottom (sediment) boundary, the sediment oxygen demand and NH_4^+ fluxes are calculated from the PON fluxes (which includes phytoplankton, zooplankton, and detritus) reaching the bottom. Phosphorus is not included in the model yet, since phosphate limitation is limited to the oligohaline bay and during the spring/winter seasons, while in the summer when hypoxia is the greatest concern, nitrogen is the primary limiting nutrient (Fisher et al., 1999). Work toward implementing the phosphorus cycle within the model is planned for the near future (see section 4.5). The original *Ches*ROMS-

ECB model has been shown to simulate Chesapeake Bay hydrodynamics and biogeochemical processes quite well (Feng et al., 2015); however, a number of modifications have been subsequently made to the original equations and parameter choices in order to improve model-data agreement. These are described in detail below.

To improve model-data comparisons for oxygen concentrations and PP in the polyhaline Chesapeake Bay, the light attenuation formulation in *Ches*ROMS-ECB was reassessed. Specifically, an underestimation of light attenuation in the polyhaline Bay was causing an overestimation of PP and oxygen. An analysis of historical CBP observations suggested that this was at least partially because the model was underestimating observed ISS by 4 mg L^{-1}. As a result, a 4 mg L^{-1} ISS wash load was added throughout the Bay. In addition, the factor converting organic suspended solids from g-C m^{-3} to g m^{-3} was changed from 2 (Feng et al., 2015) to 2.9 (Cerco & Noel, 2017). Because the historical CBP observations indicated that the lowest 25th percentile of K_D in the polyhaline Bay ranges from 0.55 to 0.75 m^{-1}, the minimum allowed value for K_D was set to 0.6 m^{-1}, as in Irby et al. (2018). Finally, the Jerlov water type (Jerlov, 1976; Paulson & Simpson, 1977) was increased to coastal waters (type 3).

To replicate the seasonal cycles of biogeochemical variables in *Ches*ROMS-ECB more realistically, temperature dependence was added to multiple biogeochemical processes, such as phytoplankton growth rate, zooplankton grazing rate, and the decomposition rate of organic matter (Table A1). The maximum phytoplankton growth rate is constant for temperatures ≤20 °C (as observed by Lomas et al., 2002) and increases exponentially at higher temperatures. Specifically, the rate at 20 °C is 2.15 d^{-1} (as in Feng et al., 2015) and reaches 3.5 d^{-1} at 30 °C. Zooplankton grazing is another highly temperature dependent estuarine process. A function based on a natural log of Q10 of 2.1 was chosen, which is derived from the community respiration study in Lomas et al. (2002). (Q10 is a measure of the temperature sensitivity of a biological/chemical reaction rate due to an increase in temperature by 10 °C.) In addition, remineralization and solubilization are important microbial activities that account for the decomposition of detrital nitrogen and carbon in *Ches*ROMS-ECB. Like metabolic activities of most organisms, bacterial productivity undergoes an exponential relationship with environmental temperature, due to enzyme activity in the Chesapeake Bay (Shiah & Ducklow, 1994). The detrital nitrogen and carbon remineralization and solubilization rates were thus modified from constant values to rates with Q10s of 2.1 (Lomas et al., 2002). All parameterization modifications were first tested independently, and then were integrated together for a combined model-skill assessment with in situ CBP data (see Online Supporting Information for skill assessment results).

2.3. Nitrogen Inputs to *Ches*ROMS-ECB

In an attempt to generate more realistic simulations of nitrogen cycling within the Chesapeake Bay than Feng et al. (2015), nitrogen inputs to the Bay were reexamined by (i) using watershed nitrogen inputs from the CBP Watershed Model, (ii) nudging to oceanic NH_4^+ and NO_3^- data along the coastal open boundary, and (iii) including atmospheric nitrogen deposition. These three inputs are described in detail below.

2.3.1. Terrestrial Inputs

As in Irby et al. (2018) watershed inputs of freshwater, nitrogen, and inorganic sediment (including both point source and nonpoint source inputs) were derived from the Phase 5.3.2 CBP Watershed Model (CBPWM; Shenk & Linker, 2013). The CBPWM includes ~1,000 model segments with an average size of 170 m^2, 237 hydrology calibration stations, and 13 types of land use that change hourly with time (USEPA, 2010b). Simulated hydrology and water quality variables are calibrated using station measurements (USEPA, 2010c).

In this study, daily estimates of CBPWM freshwater flow, NH_4^+, NO_3^-, DON, and sediments were used as terrestrial inputs to *Ches*ROMS-ECB. Median values of CBPWM DIN (NH_4^+ + NO_3^-) inputs to the Bay range from ~400 × 10^6 g-N d^{-1} during the spring freshet, to ~100 × 10^6 g-N d^{-1} in the summer (Figure 2a), with large interannual variability for the four study years (2002–2005; Table 1). Semilabile DON inputs were computed as the total biological oxygen demand plus 80% of the phytoplankton nitrogen. The refractory DON input was set to be 40% of the total refractory organic nitrogen from the CBPWM. The rest of the refractory organic nitrogen (60%) and phytoplankton nitrogen (20%) was assumed to enter the Bay as PON (Irby, 2017; Irby et al., 2018; Shenk & Linker, 2013). Although carbon cycling was not the focus of this study, carbon inputs (dissolved and particulate organic carbon and dissolved inorganic carbon) were obtained from Tian et al. (2015).

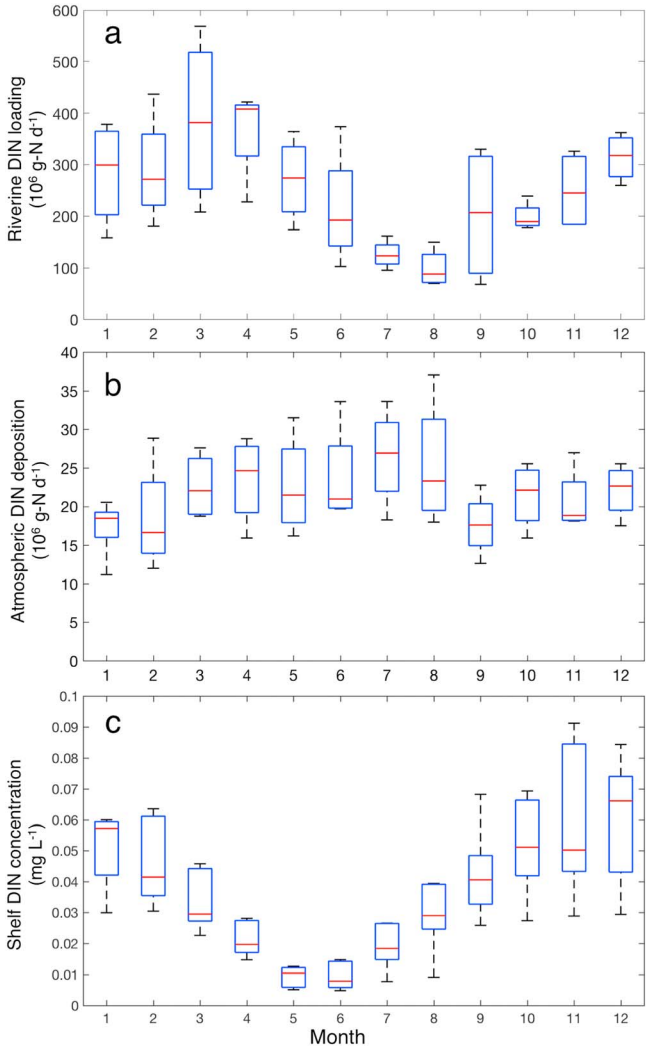

Figure 2. Average seasonality of dissolved inorganic nitrogen (DIN) inputs to *Ches*ROMS-ECB: (a) riverine DIN loading, (b) direct atmospheric DIN deposition, and (c) open boundary climatological DIN concentrations (interpolation from Melrose et al., 2015 data set). The red lines show median values, while the bottom and top edges of the blue boxes indicate the 25th and 75th percentiles, respectively. The whiskers extend to the most extreme data points.

2.3.2. Atmospheric Inputs

Because direct atmospheric deposition of DIN accounts for a significant fraction of the total DIN inputs to the Chesapeake Bay (Linker et al., 2013), an important model improvement was to include this as a source of DIN to the estuary. As is the case for the CBP's Water Quality Sediment Transport Model (Cerco & Noel, 2017), estimates of atmospheric DIN deposition were obtained from a combination of two different models: a regression model for wet deposition (Grimm, 2017; Grimm & Lynch, 2005) and a continental-scale Community Multiscale Air Quality model (CMAQ version 5.0.2, Appel et al., 2013; Gantt et al., 2015; St-Laurent et al., 2017) for dry deposition. Because the concentration of DON in wet deposition (50 mg m^{-3}; Keene et al., 2002) over the Bay is much smaller than that of DIN (400–500 mg m^{-3}; USEPA, 2010a), DON deposition is assumed to be negligible as in Grimm (2017).

Wet atmospheric deposition estimates used in this study were provided by the CBP. Specifically, their Phase 6 regression model for wet nitrogen deposition (Grimm, 2017) was refined from previous versions developed for the Chesapeake Bay watershed (Grimm & Lynch, 2005) by taking local emissions (i.e., local livestock production and fertilizer application to cropland) into consideration. Overall, the model development focused primarily on using long-term and seasonal trends in precipitation chemistry (i.e., NH_4^+ and NO_3^- concentrations and precipitation volume), land use, and local emission data as predictors selected for a stepwise linear least squares regression model (Grimm, 2017). Daily precipitation records over 1984–2014 were collected from 85 of the National Atmospheric Deposition Program, the National Trends Network, and the Pennsylvania Atmospheric Deposition Monitoring Network stations. In addition, Grimm (2017) used local land usage information from National Land Cover Data, local ammonia (NH_3), and nitrous oxide (NO_x) emissions from the National Emission Inventory database to improve the accuracy of daily NH_4^+ and NO_3^- wet deposition estimates. The daily wet DIN deposition rates were first calculated within the cells of a uniform 5-km grid overlaying the CBPWM domain, and then area-weighted to each land modeling segment or water quality management unit polygon employed by the Phase 6 Watershed Modeling Program. As part of this study, the segments positioned over the Chesapeake Bay surface water were used to provide estimates of wet deposition for each *Ches*ROMS-ECB grid cell using the nearest-neighbor method.

Monthly averaged dry DIN deposition estimates were obtained from CMAQ, an open-source numerical air quality model that simulates the atmospheric transport, chemical reactions, and emissions of various airborne gases, particles, and pollutants. The meteorological information derived from the Weather Research and Forecasting 3.4 model (Skamarock et al., 2008) and CB05TU chemistry mechanisms (Sarwar et al., 2013) are required inputs for CMAQ. The horizontal resolution of the NH_4^+ and NO_3^- deposition fields is 12 km. The

Table 1
Inputs of Dissolved Inorganic Nitrogen (DIN) to the Chesapeake Bay From Direct Atmospheric Deposition and Riverine Loading

	Average	2002 dry[a]	2003 wet	2004 wet	2005 normal
Atmospheric DIN inputs (Gg-N yr^{-1})	8.0	7.7	9.3	7.2	7.9
Riverine DIN inputs (Gg-N yr^{-1})	91	73	120	88	83
100 [a] atmospheric/riverine (%)	8.8	10.5	7.7	8.2	9.5

[a]Definitions of dry and wet years are based on annual riverine discharge to the Chesapeake Bay.

Table 2
List of Dissolved Inorganic Nitrogen (DIN) Input Sensitivity Experiments

Simulations	Atmospheric DIN inputs	Coastal DIN inputs	Riverine DIN inputs
Reference run	Realistic[a]	Realistic	Realistic
Atmospheric deposition	None[b]	Realistic	Realistic
runs (AtmN)	Double[c]	Realistic	Realistic
Coastal ocean runs	Realistic	None[b]	Realistic
(CoastalN)	Realistic	Double	Realistic
River forcing runs (ΔRiverN)	Realistic	Realistic	Δ↓[d] in DIN
	Realistic	Realistic	Δ↑in DIN

[a]"Realistic" refers to realistic inputs (nudging at open boundary, total riverine DIN inputs, or total direct atmospheric DIN deposition). [b]"None" denotes no inputs: nudging to zero DIN concentration at the open boundary or no direct atmospheric deposition. [c]"Double" denotes doubled direct atmospheric deposition or nudging to doubled DIN concentrations at the open boundary. [d]Δ↓ denotes that river inputs are reduced by the amount of atmospheric DIN deposition, that is, ~9%.

CMAQ grid points positioned over the Chesapeake Bay surface water were used for providing estimates of dry deposition for each *Ches*ROMS-ECB grid cell using the nearest-neighbor method. This monthly dry atmospheric deposition of DIN was then downscaled to daily inputs through linear interpolation. On average, dry plus wet atmospheric deposition of DIN accounts for ~10% of the riverine DIN inputs to the Chesapeake Bay, with this percentage being highest during dry years (e.g., 2002; Table 1) and in dry times of year (i.e., summer; Figures 2a and 2b).

2.3.3. Coastal Inputs

In this study, a passive-active open boundary condition (RadNud; Marchesiello et al., 2001) is used for temperature, salinity, NH_4^+, NO_3^-, oxygen, and DON. When fluxes are directed outward across the boundary, the model employs a radiation condition (passive), which is derived from a two-dimensional wave equation. As a result, the radiation boundary condition is calculated from the interior solution, propagating through the boundary as a wave. However, when fluxes are directed into the model domain from outside the boundary, the model employs a nudging condition (active). In this case the model results within the nudging region are nudged toward externally specified tracer concentrations with a nudging time scale of 15 hr. This combined radiation-nudging boundary condition is sufficient for maintaining stability (Marchesiello et al., 2001).

To improve the realism of simulated inorganic nitrogen exchange with the continental shelf, *Ches*ROMS-ECB was nudged to oceanic NH_4^+ and NO_3^- data along the outer boundary of the model domain (Figure 1), in the Middle Atlantic Bight. In situ NH_4^+ and NO_3^- data were obtained from the Ocean Acidification Data Stewardship Project data sets (https://www.nodc.noaa.gov/oceanacidification/data/; 22 cruises from 2009 to 2016) and additional cruise data (Filippino et al., 2009; five cruises from 2005 to 2006) within the domain 35.8°–38.5°N, 74.1°–76.0°W. Because the in situ data were sparsely distributed in time over the past decade, they were averaged to obtain monthly NH_4^+ and NO_3^- climatologies for the months when the most data were available: February, May, June, August, and November. Since the distribution of measurements was also spatially sparse, NH_4^+ and NO_3^- data were horizontally averaged over the model open boundary, but vertical variations were retained. The NH_4^+ and NO_3^- data in each of the 5 months were gridded onto standard 5–10 m depth intervals to obtain vertical NH_4^+ and NO_3^- profiles. These vertical profiles were then linearly interpolated to the bottom of the model grid. Only data from the upper 40 m of the water column were used for nudging, to assure consistency with the bathymetry along the model open boundary. Finally, to obtain a complete seasonal cycle of DIN along the open boundary (Figure 2c), the existing 5 months of data were interpolated to cover the full year.

In addition to nudging modeled DIN concentrations to observations at the open boundary, model estimates of dissolved organic matter were also nudged to observed estimates. Refractory DON concentrations along the open boundary were nudged to a value of 0.05 mg L^{-1}, assuming refractory dissolved organic carbon (DOC) concentrations of 0.75 mg L^{-1} and a C:N ratio of 15:1 (Fisher et al., 1998). Semilabile DOC concentrations were estimated by subtracting the constant refractory DOC (0.75 mg L^{-1}) from estimates of total DOC derived from a satellite DOC algorithm developed for the Middle Atlantic Bight (Mannino et al., 2016). Finally, a C:N ratio of 12:1 was used to estimate semilabile DON concentrations along the open boundary (Feng et al., 2015).

2.4. Model Experiments: Reference Run and Experimental Scenarios

A reference simulation was conducted to represent January 2001 to December 2005, incorporating nitrogen inputs from all three sources (watershed, atmosphere, and coastal ocean). The first year was considered to be a spin up year, and only 2002–2005 results were analyzed. These specific 4 years were chosen, as they represent a combination of dry (2002), wet (2003–2004), and normal (2005) years, and because CMAQ results (St-Laurent et al., 2017) are not available prior to 2002.

This reference simulation was compared to the results of three sensitivity experiments (AtmN, CoastalN, and ΔRiverN; Table 2) in order to assess the relative impact of nitrogen from all three sources on PP and oxygen

concentrations in Chesapeake Bay. For each sensitivity test, only one specific source of DIN was increased or reduced, while the other two sources remained the same as the reference simulation. Specifically, the sensitivity experiments included turning off and doubling atmospheric nitrogen deposition (AtmN) and setting the DIN concentrations along the open boundary to 0 and 200% of the baseline concentrations used in the reference run (CoastalN). To quantify the relative impacts of DIN from the atmosphere and continental shelf to those from land, a set of riverine DIN experiments was also conducted (ΔRiverN). These included reducing and increasing the riverine DIN loadings by the same amounts as was done in the atmospheric deposition experiments via modifying the daily riverine DIN concentrations, but keeping the freshwater discharge the same. Thus, in 2002, riverine DIN was reduced by Δ = atmospheric inputs/riverine inputs = 10.5%, whereas in 2003, riverine DIN was reduced by Δ = 7.7% (Table 2). All experiments were run from 1 January 2001 to 31 December 2005, as in the reference simulation.

A red-green-blue (RGB) primary color diagram was used to assist with visualization of the impacts of all three sensitivity experiments simultaneously. In each model grid cell (i and j), the changes in bottom DO resulting from the AtmN experiments are averaged and assigned to variable "R." Similarly, the averaged impact due to the ΔRiverN experiments is set to "G," and the averaged difference caused by the CoastalN experiments is set to "B." Then R, G, or B is each normalized to the maximum value among them (e.g., R′ = R/max [R, G, B]). The color of the grid cell (i and j) was then represented by the combination of these three numbers R′, G′, and B′. In this way, the RGB color of each grid cell within the model domain is calculated to illustrate the relative impacts of all three sensitivity experiments over the entire Chesapeake Bay. For example, red represents a 100% impact from atmospheric DIN deposition, while white means all three experiments are equally important in explaining the estimated changes in bottom DO.

3. Results

3.1. Reference Run: Along-Bay Distributions and Skill Assessment

To evaluate model skill, results from the reference run were extensively compared to CBP observations along a transect down the main channel of the Chesapeake Bay (Figure 1). For ease of comparison (Figure 3), the main stem is divided into three regions, that is, the oligohaline (defined as the region with average surface salinity $<$5 psu), mesohaline (5 psu $<$ surface salinity $<$ 15 psu), and polyhaline (surface salinity $>$ 15 psu). The salinity field is generally well captured by the model in both summer and winter throughout all three regions (±9% error, Figures 3a and 3b and supporting information), though slightly overestimates observed salinity in the southern mesohaline in winter.

The along-Bay DIN pattern is also reproduced well throughout the bay, though again minor discrepancies exist (Figures 3c and 3d). Both observed and modeled DIN concentrations peak at the head of the Bay (~1.1–1.4 mg L^{-1}) and decrease downstream, reaching concentrations less than 0.14 mg L^{-1} at the Bay mouth. Overall, summer DIN is ~0.28 mg L^{-1} lower than that in the winter. In both seasons, the model successfully reproduces the observed well-mixed conditions in the oligohaline bay, with only minor overestimates of summer DIN (by ~0.14 mg L^{-1}, ~6%). In the northern mesohaline Bay, modeled DIN concentrations agree with observations well in the upper water column but slightly underestimate the vertical gradients of DIN in the winter (Figure 3d). Throughout the southern mesohaline and polyhaline bay, the model simulates the spatial structure of DIN very well in both the summer and winter.

Model estimates of DON and PON reproduce the main stem CBP observations relatively well, though concentrations are slightly too high in the summer and too low in winter (Figures 3e and 3f). Observed concentrations of DON are highest in the mesohaline bay in both seasons with relatively small vertical gradients. Modeled DON agrees with DON concentrations and the vertical structures in the polyhaline Bay relatively well in both seasons (Figures 3e and 3f). However, the model underestimates the maximum DON concentrations in the mesohaline Bay at some stations by up to 0.07 mg L^{-1} and overestimates DON in the oligohaline bay by ~0.04 mg L^{-1} in the summer, and the bias goes up to 0.14 mg L^{-1} in the winter. PON, defined in the model as phytoplankton + zooplankton + detritus, is generally higher at the surface (Figures 3g and 3h) where light stimulates phytoplankton growth, except in the oligohaline bay where high inorganic sediment concentrations reduce light availability and thus DIN remains high (Figures 3c and 3d). The model reproduces summer PON relatively well throughout the bay, with an ~0.07 mg L^{-1} bias (+20%) in the surface mesohaline waters. In the mesohaline bay, summer PON has a sharp vertical gradient, which

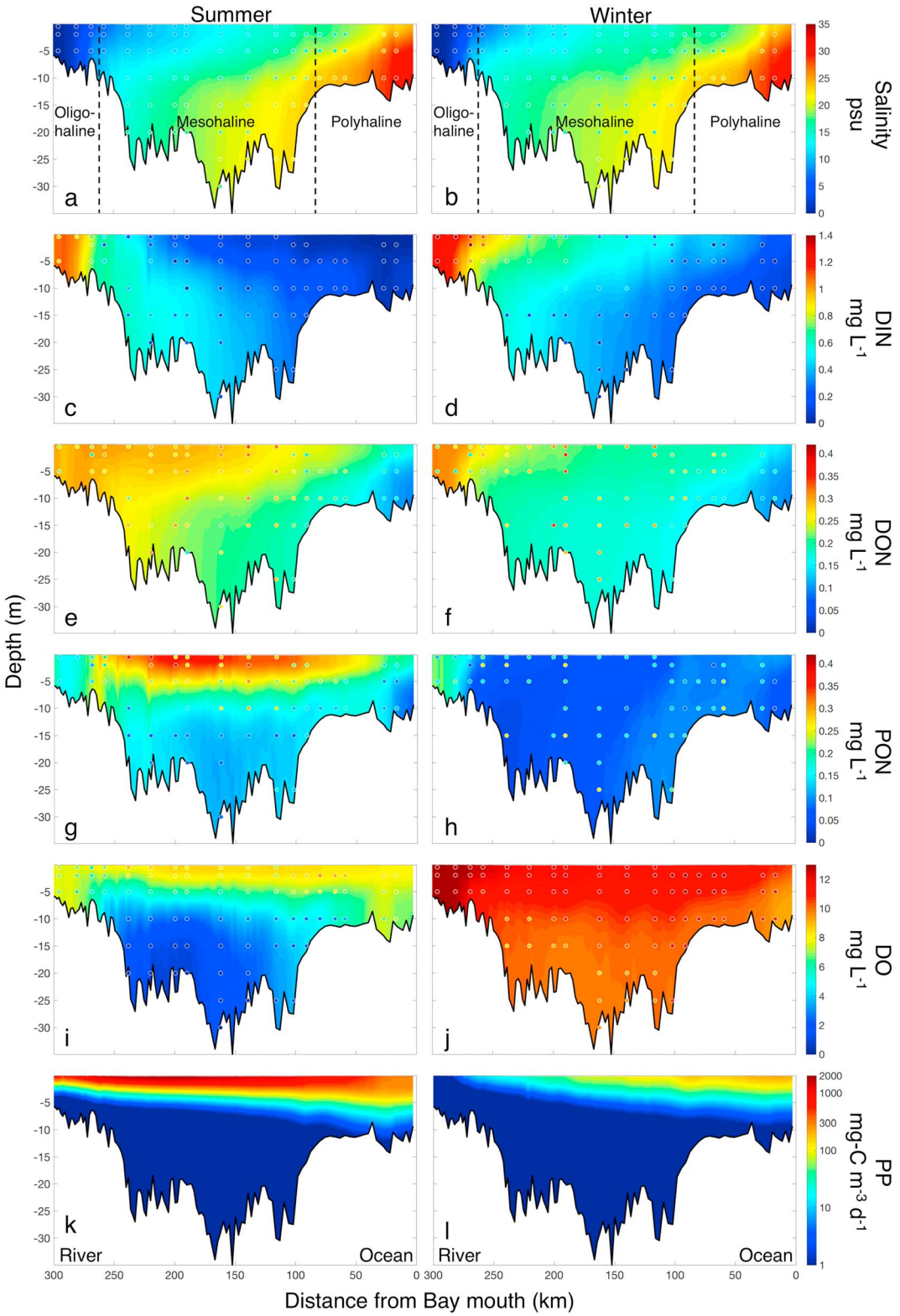

Figure 3. Four-year (2002–2005) averages of (a and b) salinity, (c and d) dissolved inorganic nitrogen, (e and f) dissolved organic nitrogen, (g and h) particulate organic nitrogen, (i and j) dissolved oxygen, and (k and l) primary production shown for the summer (a, c, e, g, i, and k) and winter (b, d, f, h, j, and l). The colored contours represent model results; the circles represent Chesapeake Bay Program observations.

Table 3
Absolute and Percent Difference in Depth-Averaged Dissolved Inorganic Nitrogen (DIN) Between the Three Sensitivity Experiments (Table 1) and the Reference Run in the Mainstem Bay[a]

	Absolute difference (10^{-2} mg L^{-1})					Percent difference (%)				
Seasons	Annual	Spring	Summer	Fall	Winter	Annual	Spring	Summer	Fall	Winter
AtmN	2.0	2.2	1.4	1.8	2.5	4.7	4.8	4.2	4.8	4.9
ΔRiverN	2.8	3.9	2.2	2.0	3.4	6.7	8.4	6.6	5.2	6.5
CoastalN	1.1	1.7	0.8	0.7	1.4	2.8	3.7	2.5	1.9	2.8

[a]Results are computed along the main stem transect between stations CB3.3C and CB6.2 (Figure 1), where hypoxia is the most prevalent. Results are computed for the average of the two sensitivity experiments (DIN increase and DIN decrease tests). For example, the absolute and percent differences in depth-averaged DIN resulting from the AtmN experiment are calculated as

$$\Delta DIN_{+AtmN} = \text{abs}\left(DIN_{reference} - DIN_{+AtmN}\right).$$

$$\Delta DIN_{-AtmN} = \text{abs}\left(DIN_{reference} - DIN_{-AtmN}\right).$$

$$\text{Absolute } \Delta DIN_{AtmN} = \frac{\Delta DIN_{+AtmN} + \Delta DIN_{-AtmN}}{2}.$$

$$\text{Percent } \Delta DIN_{AtmN} = \frac{\text{Absolute } \Delta DIN_{AtmN}}{DIN_{reference}} \times 100\%.$$

is also well captured by the model. During the winter, the model underestimates PON throughout most of the bay; however, the evenly distributed horizontal and vertical structure of PON is reproduced successfully.

The model simulates the distribution of observed oxygen well throughout the water column (Figures 3i and 3j and supporting information, ~3% overall error). The 4-year average of modeled oxygen concentrations range between 1–9 mg L^{-1} and 8–13 mg L^{-1} in the summer and winter, respectively. In both the model results and the observations, the vertical gradient during the summer is much larger than that in the winter and is larger in the mesohaline bay than the oligohaline or polyhaline bay, agreeing well with temporally averaged measurements in both seasons. Although there is a minor bias (1–2 mg L^{-1}) between the model and observation in the surface water of the mesohaline bay in the summer, the subsurface oxygen concentrations and sharp vertical gradients are both simulated well. During the winter, DO concentrations and vertical gradients are captured well by the model throughout most of the bay, although modeled bottom DO concentrations are biased high (~1 mg L^{-1}) in the deepest portions of the main stem. Most notably, the model successfully captures the large volume of hypoxic water in the deep trench during the summer.

Modeled PP is highest at the surface (up to 2,000 and 3,00 mg-C m^{-3} d^{-1} in the summer and winter, respectively) and decreases exponentially to zero within the first 3–10 m of the water column in both seasons (Figures 3k and 3l). In the polyhaline bay, PP penetrates deeper in to the water column than the oligohaline and mesohaline bay throughout the year. Summer PP peaks in the mesohaline bay where nutrients and light are both sufficient for growth (Harding et al., 2002), while surface production in the winter is the greatest in the polyhaline Bay. Although PP data are not available in the CBP Water Quality Monitoring database, the modeled estimates are qualitatively consistent with other in situ data (Harding et al., 2002) and satellite estimates (Son et al., 2014).

Additional quantitative skill metrics (Hofmann et al., 2008; Jolliff et al., 2009) were also computed to evaluate how well the reference run reproduced the CBP data. These additional results are provided in the Online supporting information and further demonstrate the reasonable skill of the modeling system.

3.2. Sensitivity Experiments: Seasonal Results in the Mainstem Mesohaline Bay

Each of the three DIN sources to the Chesapeake Bay, that is, atmospheric deposition, coastal inputs, and riverine loading, causes varying impacts on depth-averaged DIN concentrations (Table 3), depth-integrated PP (Table 4), and bottom DO (Table 5) within the main stem mesohaline region of the bay where hypoxia is of greatest concern. In this region, the ΔRiverN experiment results in a larger change in 4-year averaged

Table 4
Absolute and Percent Difference in Depth-Integrated Primary Production Between the Three Sensitivity Experiments (Table 1) and the Reference Run in the Mainstem Bay[a]

	Absolute difference (mg-C m^{-2} d^{-1})					Percent difference (%)				
Seasons	Annual	Spring	Summer	Fall	Winter	Annual	Spring	Summer	Fall	Winter
AtmN	24	16	62	16	2.7	2.2	1.5	2.6	2.1	1.7
ΔRiverN	29	20	81	13	2.2	2.6	1.9	3.3	1.7	1.3
CoastalN	10	6.4	28	6.7	0.8	0.9	0.6	1.1	0.9	0.5

[a]Results are computed along the main stem transect between stations CB3.3C and CB6.2 (Figure 1), where hypoxia is most prevalent. Results are computed for the average of the two sensitivity experiments (dissolved inorganic nitrogen [DIN] increase and DIN decrease tests).

DIN concentrations (0.03 mg L^{-1}) than either the AtmN experiment (0.02 mg L^{-1}) or the CoastalN experiment (0.01 mg L^{-1}; Table 3). In terms of annual average PP, the AtmN and ΔRiverN experiments have greater impacts (24 and 29 mg-C m^{-2} d^{-1}, respectively) than the experiment with modified coastal DIN inputs (10 mg-C m^{-2} d^{-1}), for both absolute and percent difference (Table 4). In contrast, the three experiments produce very similar annual average changes in bottom DO concentrations, although the CoastalN experiment results in a slightly greater change (0.1 mg L^{-1}; Table 5).

Overall, the three sensitivity experiments cause differences in production and bottom DO that are largest in the summer (Tables 4 and 5), while the impact on depth-averaged DIN concentrations are greatest in the spring and/or winter (Table 3). The summertime changes in depth-integrated PP in this main stem mesohaline region are higher than in other seasons: 2.6%, 3.3%, and 1.1%, resulting from the AtmN, ΔRiverN, and CoastalN experiments, respectively (Table 4), while changes in depth-averaged spring DIN concentrations are somewhat higher: 4.8%, 8.4%, and 3.7% for the three experiments, respectively (Table 3). During other seasons of the year, the percent change in bottom DO resulting from these sensitivity experiments is much lower (<2%) than those in the summer (~9% for all three experiments, Table 5). For this reason, the following sections focus on providing a more detailed examination of the sensitivity experiment results occurring in summer.

3.3. Sensitivity Experiments: Along-Bay Results in Summer

In general, the AtmN, CoastalN, and ΔRiverN experiments cause qualitatively similar impacts on water column DIN concentrations in the summer, though the spatial structures of these responses differ slightly (Figure 4). The AtmN experiment causes quite uniform changes in water column DIN concentrations horizontally and vertically (0.03–0.05 mg L^{-1}), except in the polyhaline region where little change occurs (Figures 4a and 4b). The ΔRiverN expriment results in relatively large differences in main stem DIN (up to 0.07–0.1 mg L^{-1}) in the uppermost 50 km of the bay, but these changes decrease downstream, reaching 0.03–0.05 mg L^{-1}throughout the mesohaline bay and nearly zero in the polyhaline regions (Figures 4c and 4d). The CoastalN experiment causes a larger impact on DIN in deeper waters (0.03 mg L^{-1}) and a smaller impact in shallow waters above the pycnocline. In addition, it has almost no influence in the upper oligohaline bay (Figures 4e and 4f).

Table 5
Absolute and Percent Difference in Bottom Dissolved Oxygen Between the Three Sensitivity Experiments (Table 1) and the Reference Run in the Mainstem Bay[a]

	Absolute difference (mg L^{-1})					Percent difference (%)				
Seasons	Annual	Spring	Summer	Fall	Winter	Annual	Spring	Summer	Fall	Winter
AtmN	0.09	0.09	0.17	0.09	0.03	1.4	1.1	8.6	1.5	0.29
ΔRiverN	0.08	0.08	0.18	0.06	0.01	1.3	1.0	9.2	1.0	0.15
CoastalN	0.10	0.12	0.16	0.07	0.05	1.6	1.6	8.5	1.3	0.49

[a]Results are computed along the main stem transect between stations CB3.3C and CB6.2 (Figure 1), where hypoxia is most prevalent. Results are computed for the average of the two sensitivity experiments (dissolved inorganic nitrogen [DIN] increase and DIN decrease tests).

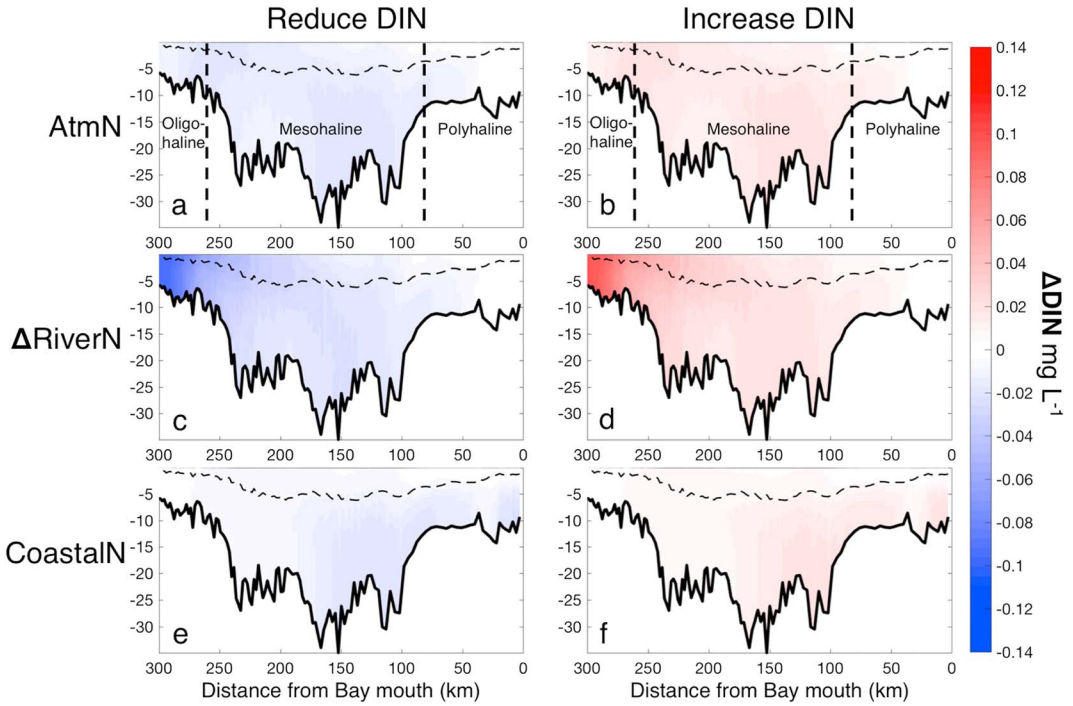

Figure 4. Four-year (2002–2005) averages of changes in dissolved inorganic nitrogen (DIN) in the summer resulting from (a and b) AtmN sensitivity experiments, (c and d) ΔRiverN sensitivity experiments, and (e and f) CoastalN sensitivity experiments; (a, c, and e) denote DIN reduction, while (b, d, and f) denote DIN increase. The dashed lines are 4-year (2002–2005) averaged summertime pycnocline (defined as in Irby et al., 2016).

The impacts of the sensitivity experiments on PP are concentrated in the uppermost 5 m of the water column and are of the same order of magnitude for all three experiments (Figure 5). As expected, increases and decreases in DIN inputs result in increases (Figures 5b, 5d, and 5f) and decreases in PP (Figure 5a, 5c, and 5e), respectively. In the turbidity maximum zone, PP barely changes regardless of which DIN input is modified. Both the AtmN and ΔRiverN experiments cause 60–80 mg-C m^{-3} d^{-1} differences in PP throughout the mesohaline Bay and result in 20–40 mg-C m^{-3} d^{-1} changes in the polyhaline bay. However, the ΔRiverN experiment has a slightly greater impact than the AtmN experiment in the mesohaline bay, and the AtmN experiment results in a little more changes in the polyhaline bay than the ΔRiverN test. Although the CoastalN impacts production less than either of the other two experiments in the northern mesohaline bay, it causes larger and deeper changes in PP throughout the polyhaline bay (~50 mg-C m^{-3} d^{-1} and ~10 m, respectively).

Dissolved oxygen is changed by up to 0.3 mg L^{-1} in the summer for all three sensitivity experiments (Figure 6). Generally, if DIN inputs are reduced, DO decreases at the surface and increases below the pycnocline, and vice versa. Both the AtmN and ΔRiverN experiments cause an ~0.1 mg L^{-1} change in surface DO in the southern mesohaline and polyhaline bay, while a smaller increase is observed in the CoastalN experiments. Below the pycnocline, DO concentrations barely change in the oligohaline bay regardless of which DIN input is modified; however, in the mesohaline bay, changes of 0.1–0.3 mg L^{-1} result from each experiment. Specifically, the impacts on DO are greatest in the deep trench (up to 0.3 mg L^{-1}). Most notably, the CoastalN experiment impacts DO ~0.1 mg L^{-1} less in the northern mesohaline bay and ~0.1 mg L^{-1} more in the polyhaline region than either of the other two experiments.

Overall, the three sensitivity experiments have an equally important influence on the cumulative hypoxic volume (CHV) of the Chesapeake Bay (Table 6) (CHV is calculated by integrating the volume of all grid cells with DO less than a certain threshold concentration, e.g., 5 mg L^{-1}, as described in Bever et al., 2013). In general, the impact on CHV resulting from the AtmN and ΔRiverN experiments becomes larger than that from the CoastalN experiment as the DO threshold defining "hypoxia" is decreased. For example, at DO $<$5 mg L^{-1}, modifying either atmospheric or riverine DIN inputs changes CHV less than altering the coastal DIN inputs

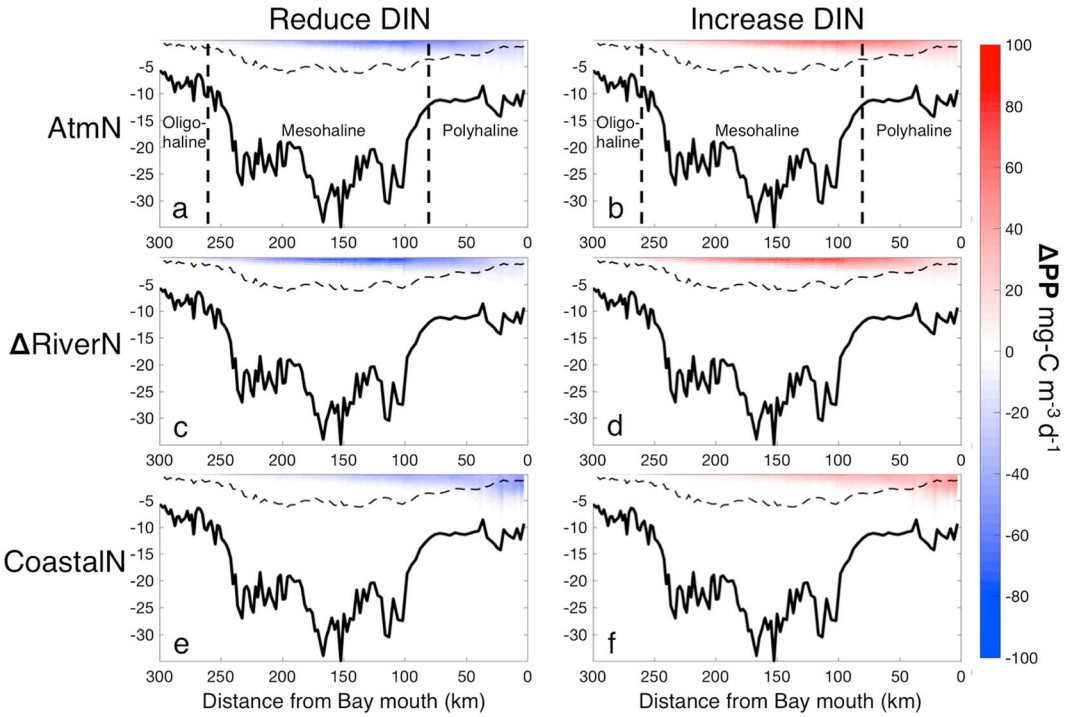

Figure 5. Four-year (2002–2005) averages of changes in primary production in the summer resulting from (a and b) AtmN sensitivity experiments, (c and d) ΔRiverN sensitivity experiments, and (e and f) CoastalN sensitivity experiments; (a, c, and e) denote dissolved inorganic nitrogen (DIN) reduction, while (b, d, and f) denote DIN increase. The dashed lines are 4-year (2002–2005) averaged summertime pycnocline.

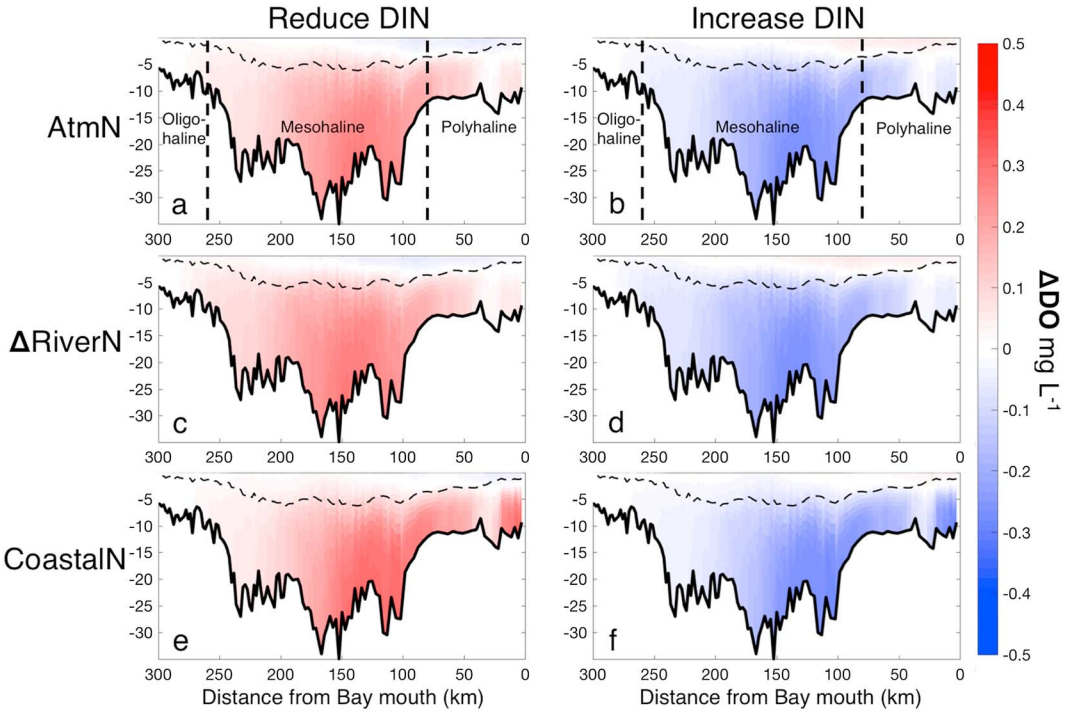

Figure 6. Four-year (2002–2005) averages of changes in dissolved oxygen in the summer resulting from (a and b) AtmN sensitivity experiments, (c and d) ΔRiverN sensitivity experiments, and (e and f) CoastalN sensitivity experiments; (a, c, and e) denote dissolved inorganic nitrogen (DIN) reduction, while (b, d, and f) denote DIN increase. The dashed lines are 4-year (2002–2005) averaged summertime pycnocline.

Table 6
Absolute and Percent Difference in Cumulative Hypoxic Volumes Between the Three Sensitivity Experiments (Table 1) and the Reference Run

	Absolute difference (km^3 d)[a]				Percent difference (%)[a]			
DO level (mg L^{-1})	<5	<2	<1	<0.2	<5	<2	<1	<0.2
AtmN	94	48	31	11	5.6	11	16	23
ΔRiverN	93	51	34	13	5.6	12	17	26
CoastalN	95	43	27	9	5.7	10	14	19

[a]In each case results are shown for the average of the two sensitivity experiments (dissolved inorganic nitrogen [DIN] increase and DIN decrease tests). The differences in hypoxic volume are calculated assuming various thresholds for hypoxia: dissolved oxygen (DO) < 5/2/1/0.2 mg L^{-1}.

(by 1–2 km^3 d); this has a larger impact in the polyhaline Bay where DO concentrations are relatively high (Figure 3i). However, at DO <0.2 mg L^{-1}, the AtmN and ΔRiverN experiments have 4% and 7% greater impacts on CHV than does the CoastalN experiment, respectively, since these lowest DO concentrations occur in the mesohaline bay far from the coastal boundary (Figure 3i).

3.4. Sensitivity Experiments: Dry Versus Wet Years

The impact of changes in nitrogen inputs on main stem DIN concentrations can depend on whether a year is particularly dry (e.g., 2002) or wet (e.g., 2003). Depth-averaged concentrations of DIN are examined here, in order to include impacts of both surface (AtmN and ΔRiverN) and bottom DIN (CoastalN) sources. In the AtmN and CoastalN experiments, differences in depth-averaged DIN concentrations along the main stem are relatively evenly distributed throughout the bay (0–0.02 mg L^{-1}) and are similar for both dry and wet years (Figures 7a and 7c). The impact on DIN along the main stem resulting from the ΔRiverN experiment peaks in the oligohaline bay (~300 km away from the Bay mouth) and generally decreases to nearly zero in the polyhaline bay in both dry and wet years (Figure 7b). In contrast to the other two sensitivity experiments, in the oligohaline bay, the ΔRiverN experiment results in an ~0.05 mg L^{-1} greater difference in the dry year compared to that in the wet year (Figure 7b).

In the wet year, the largest changes in depth-integrated PP resulting from the AtmN and ΔRiverN experiments are farther downstream than those in the dry year (Figures 7d and 7e). The CoastalN experiment, however, demonstrates smaller differences in impacts in dry versus wet years (Figure 7f). Depth-integrated PP increases up to 150 and 180 mg-C m^{-2} d^{-1} in the mesohaline bay during a dry year for the AtmN and ΔRiverN experiments, respectively, both decreasing upstream to zero in the turbidity maximum zone. On the contrary, these maximum changes in PP resulting from atmospheric and riverine inputs are located in the polyhaline bay in the wet year (~100 mg-C m^{-2} d^{-1}). Regardless of dry or wet conditions, the CoastalN experiment has almost no impact on depth-integrated production in the northern mesohaline and oligohaline bay (Figures 7f and 7e). However, its impacts increase gradually along the main stem to ~200 mg-C m^{-2} d^{-1} in the polyhaline bay, with slightly greater changes in the dry year (Figure 7f).

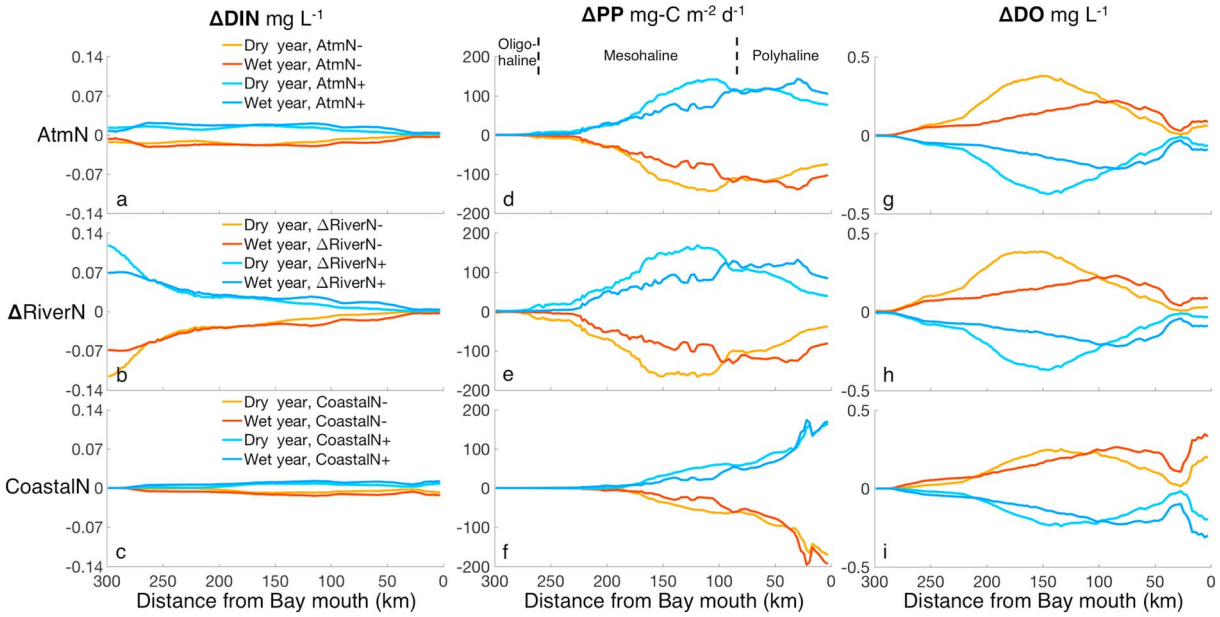

Figure 7. Impacts of three sensitivity experiments (Table 1) on (a–c) summer depth-averaged dissolved inorganic nitrogen, (d–f) depth-integrated primary production, and (g–i) bottom dissolved oxygen in the dryest year considered (2002) and the wettest year (2003); (a, d, and g) AtmN sensitivity experiments, (b, e, and h) ΔRiverN sensitivity experiments, and (c, f, and i) CoastalN sensitivity experiments.

Table 7
Reference Run Annual Dissolved Inorganic Nitrogen (DIN) Fluxes and the Changes in DIN Fluxes at the Mouth of the Bay Due to Coastal DIN Input

	DIN flux	Average	2002 dry	2003 wet	2004 wet	2005 normal
Reference run DIN flux (Gg-N yr^{-1})	Seaward flux at surface	43	13	65	56	37
	Landward flux at depth	19	12	24	22	16
	Net flux[a]	24	1	41	34	21
Changes in DIN flux due to CoastalN[b] (Gg-N yr^{-1})	ΔSeaward flux	4.4	2.3	5.9	5.4	4.0
	ΔLandward flux	5.3	4.0	6.6	6.1	4.6
	ΔNet flux[c]	−0.9	−1.7	−0.7	−0.7	−0.6

[a]Positive values imply the net flux is directed seaward. [b]In each case results are shown for the average of the two sensitivity experiments (DIN increase and DIN decrease tests). [c]Negative values imply that the net seaward flux is reduced.

The maximum impact on summer bottom DO from all three sensitivity experiments occurs in the mesohaline bay during the dry year, whereas it is located farther downstream in the polyhaline bay in the wet year (Figures 7g–7i). Specifically, for both the AtmN and ΔRiverN experiments, bottom DO is impacted by up to 0.3 mg L^{-1} in the mesohaline bay in the dry year, but the impacts are smaller (~0.15 mg L^{-1}) and farther south in the wet year. The CoastalN experiment results in slightly smaller changes in bottom DO (up to 0.2 mg L^{-1}) in the dry year; however, in the wetter year, the differences in bottom DO due to coastal DIN inputs reach up to 0.3 mg L^{-1} at the mouth of the bay. Overall, regardless of whether a year is particularly dry or wet, the results from the AtmN and ΔRiverN sensitivity experiments are very similar throughout the bay, whereas the CoastalN experiment results in a greater impact in bottom DO in the polyhaline bay (0.1–0.2 mg L^{-1}) and a smaller impact in the mesohaline bay (~0.1 mg L^{-1}) compared to the other two scenarios.

4. Discussion

4.1. Overall Bottom Oxygen Response to Atmospheric and Coastal DIN Inputs

Direct atmospheric DIN deposition is a crucial source of nutrients entering the Chesapeake Bay and causes nearly the same impact on hypoxia as the same amount of riverine DIN loading. Direct atmospheric DIN deposition fuels an additional ~100 mg-C m^{-2} d^{-1} of PP during the summer in the nutrient-limited mesohaline Bay (Figures 5b and 7d), providing more organic material as substrate for microbial decomposition and decreasing DO concentrations by up to 0.3 mg L^{-1} (Figures 6b and 7g). Similarly, decreasing riverine DIN loading by ~10% has roughly the same impact as eliminating atmospheric DIN deposition, on reducing bottom oxygen concentrations (Table 5) and CHV (Table 6) in the hypoxia-prone main stem. In particular, because the average of atmospheric DIN deposition is roughly equal to ~10% of riverine DIN inputs (Figure 2), direct atmospheric DIN deposition causes nearly the same impact on hypoxia as the same gram for gram change in riverine DIN loading. Since DIN inputs represent ~60% of the total nitrogen entering from the watershed, a 1.0 Gg-N reduction in atmospheric DIN deposition causes essentially the same increase in hypoxia as reducing 1.6 Gg-N of total nitrogen inputs from the watershed. This is critical information for coastal resource managers who must assess impacts of changes in atmospheric and riverine nitrogen loading to the bay.

Coastal DIN concentrations are also critical for understanding trends in Chesapeake Bay hypoxia and generally cause a similar impact on oxygen concentrations as direct atmospheric DIN deposition, even though the overall net DIN flux through the Chesapeake Bay mouth is directed from the Bay to the shelf (Table 7). DIN from the coastal ocean has a smaller impact than atmospheric DIN on summer PP in the mesohaline bay (~50 mg-C m^{-2} d^{-1}; Figures 5f and 7f), since coastal DIN enters the bay at the bottom of the water column via estuarine circulation, whereas DIN from the atmosphere enters at the nutrient-limited surface. However, higher coastal DIN concentrations on the shelf result in greater phytoplankton growth on the shelf and ultimately more allochthonous organic matter input entering through the bay mouth (Table 8). As a result, more oxygen is consumed when this additional organic matter is remineralized in the bay at depth. Thus, although the in situ mesohaline PP is greater when additional DIN enters from the atmosphere rather than from the coast (Table 4), the additional organic matter provided by allochthonous inputs from the coast (Table 8) causes the reduction in bottom DO to be comparable in both cases (Table 5), regardless of whether the

Table 8
Reference Run Annual Particulate Organic Nitrogen (PON) Fluxes and the Changes in PON Fluxes at the Mouth of the Bay Due to Coastal Dissolved Inorganic Nitrogen (DIN) Concentrations

	PON flux	Average	2002 dry	2003 wet	2004 wet	2005 normal
Reference run PON flux(Gg-N yr^{-1})	Seaward flux at surface	66	45	88	68	64
	Landward flux at depth	26	22	30	26	26
	Net flux[a]	40	23	58	42	38
Changes in PON flux due to CoastalN[b] (Gg-N yr^{-1})	ΔSeaward flux	4.2	4.6	3.5	4.1	4.6
	ΔLandward flux	5.5	5.0	5.1	5.7	6.3
	ΔNet flux[c]	−1.3	−0.4	−1.6	−1.6	−1.7

[a]Positive values imply the net flux is directed seaward. [b]In each case results are shown for the average of the two sensitivity experiments (DIN increase and DIN decrease tests). [c]Negative values imply the net seaward flux is reduced.

source of extra nitrogen is from the atmosphere or the shelf. Therefore, atmospheric and coastal DIN concentrations are both crucial sources of nutrients that impact Chesapeake Bay oxygen dynamics.

4.2. Seasonal Variability of Bottom Oxygen Response to Atmospheric and Coastal DIN Inputs

The impacts of changing atmospheric and coastal DIN sources on PP are modulated seasonally by both physical and biogeochemical processes. In summer, a combination of high temperatures and abundant solar radiation promotes the growth of phytoplankton (Kremer & Nixon, 1978), resulting in high rates of PP (Figure 3). Furthermore, strong spring river discharge results in strengthened stratification in the summer (Scully, 2013), which helps to keep highly productive surface layers from being mixed with more light limited subpycnocline water, maintaining the high surface production. As a result, the surface waters of the mesohaline Bay are depleted of nitrogen (Kemp et al., 2005), and thus, PP is very sensitive to changes in DIN inputs from the atmosphere and shelf during the summer (Table 4 and Figure 5). The considerable increase in production during the summer caused by the added direct atmospheric DIN and elevated shelf DIN concentrations also results in more organic material being available for microbial decomposition and ultimately enhanced oxygen consumption (thereby reducing oxygen concentrations) throughout the summer (Table 5 and Figure 6). Because DIN inputs are immediately taken up by the resident nutrient-limited phytoplankton community in the summer, DIN concentrations, in contrast, are not as strongly impacted by these summer inputs in the mesohaline bay (Figure 4) but are more strongly impacted by additional inputs in spring when nitrogen is not as limiting (Table 3).

In the winter, low temperatures and light are the primary reason for the small change in PP resulting from changes in DIN inputs. Phytoplankton growth rate in the winter is much lower than that in the summer (Eppley, 1972), and light limitation is stronger in the winter due to deeper vertical mixing (Fisher et al., 1999). As a result, the impacts of new sources of DIN on PP are smallest in winter (Table 4), whereas the impact on depth averaged DIN concentration is relatively high (Table 3) since very little of these additional DIN inputs is assimilated into organic matter at this time of year. This is true despite the fact that shelf DIN concentrations are highest in the winter (Figure 2c). These limited changes in PP coupled with the low microbial degradation rates due to the cold temperatures cause minimal changes in bottom DO in the winter.

4.3. Interannual Variability of Bottom Oxygen Response to Atmospheric and Coastal DIN Inputs

Although the impact of atmospheric DIN deposition on DIN concentration shows little interannual variability, the impacts on production and oxygen vary substantially according to whether a specific year is particularly dry or wet (Figures 7d and 7g). Specifically, in dry, low-flow years riverine DIN loading is reduced and the available DIN is assimilated in the oligohaline and northern mesohaline bay, thus providing less DIN advection to the southern mesohaline Bay (Figure 8a). Because nitrogen is therefore more limiting in the mesohaline bay in dry years, the impact of additional DIN inputs to this portion of the bay is stronger in such years. In the mesohaline bay, doubling atmospheric deposition has almost twice as great an impact on production in a dry year than a wet year (Figure 7d) and therefore twice as great an impact on bottom oxygen as well (Figure 7g). During the wet year, higher river flow carries more DIN to the mesohaline bay than in the dry year (Figure 8b) and results in the annual phytoplankton bloom and production maximum being located in more seaward regions of the bay (Figure 8d; Hagy et al., 2005, Testa & Kemp, 2014). Thus, in the wet year, instead of

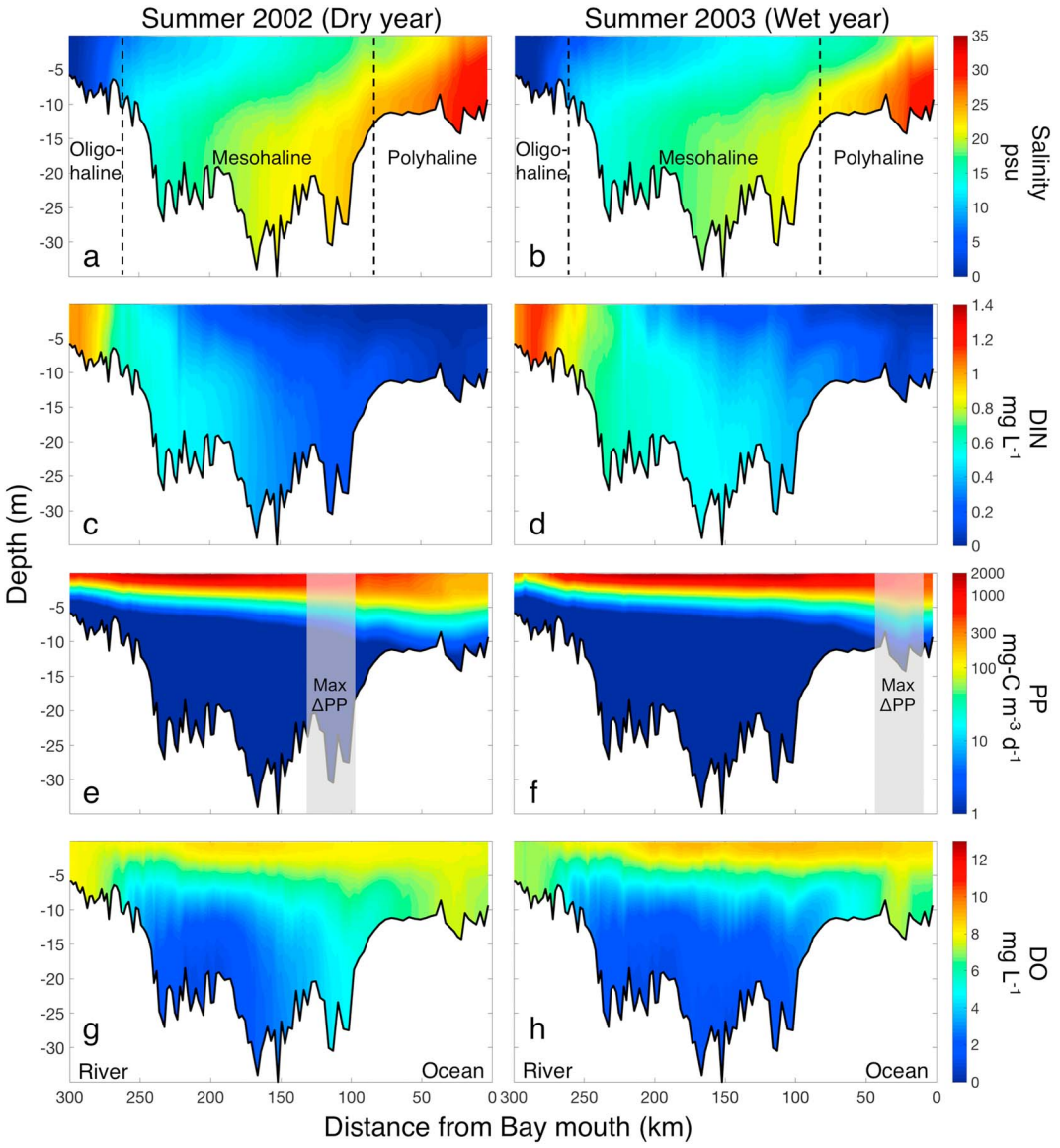

Figure 8. Model results of (a and b) salinity, (c and d) dissolved inorganic nitrogen (DIN), (e and f) primary production, and (g and h) dissolved oxygen along the main stem of the Chesapeake Bay; (a, c, e, and g) represent summer 2002 (a dry year), and (b, d, f, and h) represent summer 2003 (a wet year). The shading areas represent the locations of maximum change in primary production resulting from atmospheric DIN deposition.

the mesohaline bay being the most nutrient-limited region, the polyhaline bay becomes the most DIN-depleted. As a result, the location of maximum increase in PP and decrease in bottom oxygen due to atmospheric deposition migrates farther downstream in wet years compared to dry years. Additionally, since phytoplankton in the polyhaline bay are always nitrogen limited, the larger atmospheric DIN deposition in wetter years (Table 1) results in the impact of atmospheric deposition in the polyhaline bay being greater in wet years than dry years for both productivity and oxygen (Figures 7d and 7g).

Biogeochemical processes and estuarine circulation together determine the interannual variability associated with impacts of coastal DIN concentrations. As discussed above, in both dry and wet years, phytoplankton in the surface waters of the polyhaline bay are always the most nitrogen-limited (Figures 8a and 8b). In this region, increases in DIN due to higher DIN concentrations on the shelf are similar in both years (Figure 7c), and increases in PP in the polyhaline bay also show very little interannual variability (Figure 7f). On the contrary, the mesohaline bay is more nitrogen limited in dry years than wet years and is thus more

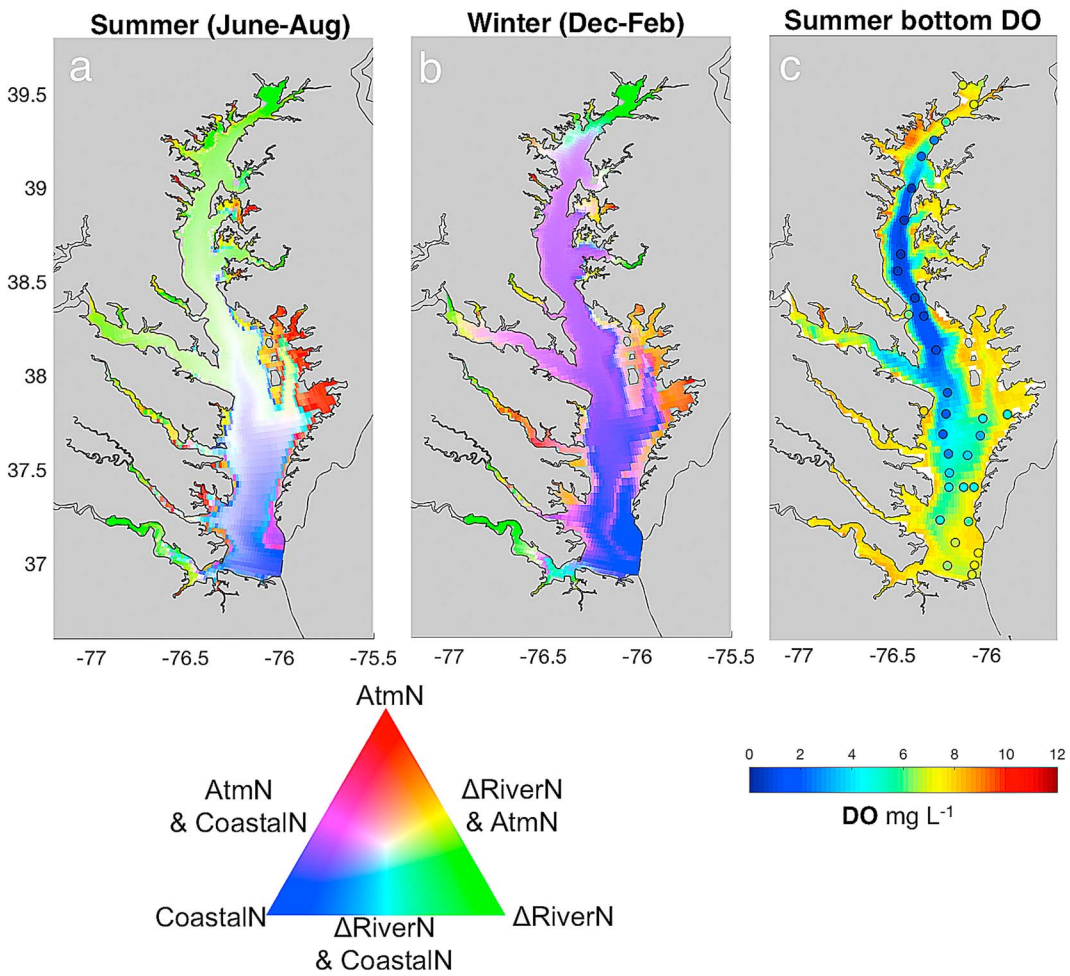

Figure 9. Relative impacts on bottom dissolved oxygen (DO) resulting from the three sensitivity experiments (Table 1) during (a) summer, (b) winter, and (c) summer bottom DO averaged over 2002–2005 (circles represent Chesapeake Bay Program observations).

sensitive to coastal DIN inputs during dry years. Thus, the increase in PP and decrease in bottom DO in the mesohaline bay are larger in dry years than wet years (Figures 7f and 7i). Estuarine dynamics theory also indicates that the exchange flow at the bay mouth increases with river discharge following a two-third power law (Geyer, 2010; Scully, 2013). Thus, during high flow years, the enhanced circulation causes a larger increase in seaward flux of low-DIN waters exiting from the Chesapeake Bay at the surface and a larger increase in landward DIN flux from the coastal ocean at depth in response to increased coastal DIN concentrations (Table 7). In addition, the larger reduction (+114%) in DO flux at depth from the shelf into the polyhaline bay results in almost doubled decreases in polyhaline bay bottom oxygen concentrations in wet years compared to dry years (Figure 7i).

4.4. Spatial Variability of Bottom Oxygen Response to Atmospheric and Coastal DIN Inputs

Dissolved inorganic nitrogen inputs from the atmosphere, coastal ocean, and rivers all impact summer hypoxia, but the locations of their largest contributions differ spatially throughout the bay. Since over 90% of freshwater inputs are from the three major rivers (i.e., the Susquehanna, Potomac, and James Rivers), riverine DIN inputs have the greatest impact on DO in the oligohaline bay and inside these largest tributaries (Figure 9a). On the contrary, atmospheric DIN deposition has the greatest impact on bottom oxygen in the shallow regions of the mesohaline bay closest to land (e.g., in the small tributaries and on the shoals) where atmospheric DIN is greatest (Schwede & Lear, 2014). In the model, only a small amount of riverine nitrogen enters the shoals from the east, leading to a minimal influence from rivers on the shallow eastern

mesohaline shoals and subsequently resulting in a larger relative impact of atmospheric nitrogen in these regions showed in red (Figure 9a). Lastly, because the polyhaline bay is most exposed to the continental shelf waters, coastal DINs have the greatest impact there. In the central portion of the bay where summer hypoxia is most prevalent, all three sources of DIN have substantial impacts on bottom oxygen (Figure 9a), with the inputs of atmospheric and coastal nitrogen being nearly equally important (Table 5).

In the winter, DIN inputs from the continental shelf strongly influence bottom oxygen concentrations throughout the majority of the bay (Figure 9b). This is partially a result of the fact that climatological DIN concentrations on the continental shelf peak in winter (Figure 2c). Additionally, enhanced estuarine circulation in the winter due to high winter river discharge (Geyer, 2010; Scully, 2013) helps extend the impacts of coastal DIN farther upstream. However, although coastal nitrogen sources have a relatively strong impact on bottom oxygen concentrations in the winter (Figure 9b), the percent impact on bottom oxygen is very small (0.49%; Table 5), since oxygen concentrations in the winter are very high.

4.5. Future Work

Although the modified *Ches*ROMS-ECB model applied in this study reproduces most physical and biogeochemical fields well, the following future efforts may further improve the model's performance and hence the realism of sensitivity experiments such as those conducted here. First, the temporal variability of PON may be improved by including more than one type of phytoplankton and zooplankton. Adding another phytoplankton species with a lower optimal temperature and a different carbon to chlorophyll ratio (Xiao & Friedrichs, 2014a, 2014b) would likely improve model estimates of bottom PON and chlorophyll during the spring in the northern mesohaline bay. Additionally, including phosphate limitation could improve the realism of the model simulations, since oceanic phosphorus and sediment phosphorus fluxes can play an important role in Chesapeake Bay nutrient cycling, especially in the oligohaline bay and spring/winter seasons when phosphorus can be more limiting than nitrogen (Kemp et al., 2005). Furthermore, incorporating a sediment-biogeochemical model could improve the estimates of oxygen and nutrients fluxes at seabed-water column interface, eventually isolating the impact on DO from sediment nutrient supply (Moriarty et al., 2017). Nudging to interannually varying DIN concentrations along the model open boundary will be important as more in situ data become available in the future.

Although in the current version of *Ches*ROMS-ECB riverine inputs to the bay are distributed to only the 10 largest tributaries (Figure 1), current work is underway to improve the realism of the locations of these freshwater inputs. In the real-world there are far more rivers and creeks exporting inorganic and organic materials to the Chesapeake Bay. Thus, increasing the number of locations where these inputs enter the model grid will make future model simulations more realistic. For example, the eastern mesohaline bay is strongly influenced by heavy fertilizer application in eastern Maryland and Virginia, so nutrients coming from surface runoff could be substantial (Ator & Denver, 2015). The addition of more localized terrestrial inputs to the model could potentially lower the importance of atmospheric DIN deposition in eastern mesohaline shoals. However, applying spatially higher-resolution atmospheric deposition products when they become available will be an important model improvement as well and could potentially increase the impact of atmospheric inputs in nearshore regions where deposition is generally largest. Lastly, including tidal wetlands in *Ches*ROMS-ECB could be important since Najjar et al. (2018) indicate that tidal wetlands play a crucial role in coastal biogeochemical cycling.

5. Summary and Conclusions

This study examines the relative impacts of two sources of DIN on Chesapeake Bay bottom oxygen concentrations: direct atmospheric DIN deposition and coastal DIN inputs at depth. Through the use of an extensively evaluated three-dimensional hydrodynamic-ECB model (Feng et al., 2015; Irby et al., 2016, 2018), direct atmospheric DIN deposition and coastal DIN concentrations are found to substantially impact Chesapeake Bay PP and DO, especially in the summer (up to 200 mg-C m^{-2} d^{-1} and 0.3 mg L^{-1}, respectively). Direct atmospheric DIN deposition causes nearly the same impact on hypoxia as the same gram for gram change in riverine DIN loading, although their spatial and temporal distributions are distinct. During dry years, increasing atmospheric DIN input causes the greatest increase in PP and the greatest reduction in bottom oxygen in the nutrient-limited mesohaline bay. These largest changes are farther downstream in wet years. The coastal ocean is another important source of DIN for the bay and has a similar impact on

Table A1
Modified Biogeochemical Parameters From Feng et al. (2015)

Description	Feng et al. (2015) value	New value used in this study	Units
Zooplankton maximum growth rate	$g_{max} = 0.3$	$g_{max} = 0.05 \times e^{0.0742 \times T}$	d^{-1}
Total suspended solids	$TSS = ISS + \eta^{*}_{C:N} \frac{P+Z+D_S+D_L}{1{,}000} \times 12$	$TSS = ISS + 4 + 2.9 \times \eta_{C:N} \frac{P+Z+D_S+D_L}{1{,}000} \times 12$	mg L^{-1}
Light attenuation	$K_D = 1.4 + 0.063[TSS] - 0.057S$ If $1.4 + 0.063[TSS] - 0.057S < 0$, then $K_D = 0.04 + 0.02486[Chl] + 0.003786\{0, 6.625\ ([DON]_{SL} + [DON]_{RF}) - 70.819\}_{max}$	$K_D = MAX\ (1.4 + 0.063[TSS] - 0.057S, 0.6)$	m^{-1}
Remineralization of large detritus	$r_{D_L} = 0.2$	$r_{D_L} = 0.05 \times e^{0.0742 \times T}$	d^{-1}
Remineralization of small detritus	$r_{D_S} = 0.2$	$r_{D_S} = 0.05 \times e^{0.0742 \times T}$	d^{-1}
Temperature dependency remineralization of semilabile DON	$\kappa_{[DON]_{SL}} = 0.07$	$\kappa_{[DON]_{SL}} = 0.0742$	$(°C)^{-1}$
Phytoplankton growth rate	$\mu_0 = 2.15$	If $T < 20$, $\mu_0 = 2.15$ If $T \geq 20$, $\mu_0 = 1.81 + e^{0.16 \times T - 4.28}$	d^{-1}

*$\eta_{C:N}$ denotes molar phytoplankton carbon : nitrogen ratio = 106/16 mol C/Mol N

summer hypoxia as direct atmospheric DIN deposition, while this coastal DIN primarily impacts hypoxia via the deposition of allochthonous material entering the bay mouth from the shelf. Spatially, the atmospheric DIN input has greatest impact on oxygen in the shoals of the bay, while coastal DIN input has greatest impact in the polyhaline bay.

When studying Chesapeake Bay eutrophication and hypoxia, researchers typically focus on riverine DIN loading, while often neglecting other potential DIN sources such as direct atmospheric DIN deposition and continental shelf DIN concentrations (Feng et al., 2015; M. Li et al., 2016). In this research, careful integration of DIN from all three of these different sources produced a more realistic simulation of biogeochemical dynamics in the Chesapeake Bay and quantified the considerable impacts that direct atmospheric DIN deposition and coastal DIN concentrations have on PP and hypoxia. Considering long-term trends in atmospheric DIN deposition is critical for demonstrating the positive estuarine impacts resulting from the success that has been made in reducing airborne pollutants (Paerl, 1997). Finally, future sea level rise, which has been predicted to increase estuarine circulation (Irby et al., 2018), also needs to be taken into account as it will likely increase the impact of coastal nitrogen fluxes on future hypoxia in Chesapeake Bay.

Acknowledgments
This work has been supported by the NASA Interdisciplinary Science Program (NNX14AF93G) and by the National Science Foundation (OCE-1259187). We thank Courtney Harris, Raleigh Hood, and Jian Shen for their helpful comments on an initial version of this manuscript and Kyle Hinson and the CBP Watershed Modeling team for providing the riverine and atmospheric input files used in this analysis. This work was performed using High Performance Computing facilities at the College of William & Mary, which were provided by contributions from the National Science Foundation, the Commonwealth of Virginia Equipment Trust Fund, and the Office of Naval Research. Model output is publicly available through W&M's ScholarWorks at https://doi.org/10.21220/gaww-m696. This paper is contribution 3751 of the Virginia Institute of Marine Science, College of William & Mary.

Appendix A: Modified *Ches*ROMS-ECB Parameters

Model parameters and formulations modified from those used in Feng et al. (2015) are listed in Table A1.

References

Appel, K. W., Pouliot, G. A., Simon, H., Sarwar, G., Pye, H. O. T., Napelenok, S. L., et al. (2013). Evaluation of dust and trace metal estimates from the community multiscale air quality (CMAQ) model version 5.0. *Geoscientific Model Development*, *6*, 883. https://doi.org/10.5194/gmd-6-883-2013

Ator, S.W., & Denver, J.M. (2015). Understanding nutrients in the Chesapeake Bay watershed and implications for management and restoration—The Eastern Shore (ver. 1.2, June 2015). U.S. Geological Survey Circular 1406, 72 p.https://doi.org/10.3133/cir1406

Bever, A. J., Friedrichs, M. A. M., Friedrichs, C. T., Scully, M. E., & Lanerolle, L. W. (2013). Combining observations and numerical model results to improve estimates of hypoxic volume within the Chesapeake Bay, USA. *Journal of Geophysical Research: Oceans*, *118*, 4924–4944. https://doi.org/10.1002/jgrc.20331

Blanton, J. O., Schwing, F. B., Weber, A. H., Pietrafesa, L. J., & Hayes, D. W. (1985). In L. P. Atkinson, D. W. Menzel, & K. A. Bush (Eds.), *Wind stress climatology in the South Atlantic Bight, in oceanography of the southeastern U.S. continental shelf*. Washington, DC, American Geophysical Union. https://doi.org/10.1029/CO002p0010

Bronk, D. A., Glibert, P. M., Malone, T. C., Banahan, S., & Sahlsten, E. (1998). Inorganic and organic nitrogen cycling in Chesapeake Bay: Autotrophic versus heterotrophic processes and relationships to carbon flux. *Aquatic Microbial Ecology*, *15*(2), 177–189. https://doi.org/10.3354/ame015177

Brown, C. A., & Ozretich, R. J. (2009). Coupling between the coastal ocean and Yaquina Bay, Oregon: Importance of oceanic inputs relative to other nitrogen sources. *Estuaries and Coasts*, *32*(2), 219–237. https://doi.org/10.1007/s12237-008-9128-6

Cerco, C. and Noel, M. (2017). The 2017 Chesapeake Bay water quality and sediment transport model. U.S. Army Engineer Waterways Experiment Station, Vicksburg MS. https://www.chesapeakebay.net/documents/2017_WQSTM_Documentation_DRAFT_5-10-17.pdf

Davis, K. A., Banas, N. S., Giddings, S. N., Siedlecki, S. A., MacCready, P., Lessard, E. J., et al. (2014). Estuary-enhanced upwelling of marine nutrients fuels coastal productivity in the U.S. Pacific Northwest. *Journal of Geophysical Research: Oceans*, *119*, 8778–8799. https://doi.org/10.1002/2014JC010248

Diaz, R. J., & Rosenberg, R. (1995). Marine benthic hypoxia: A review of its ecological effects and the behavioural responses of benthic macrofauna. *Oceanography and Marine Biology: An Annual Review*, *33*, 245–203.

Eppley, R. W. (1972). Temperature and phytoplankton growth in the sea. *Fishery Bulletin*, *70*, 1063–1085.

Feng, Y., Friedrichs, M. A., Wilkin, J., Tian, H., Yang, Q., Hofmann, E. E., et al. (2015). Chesapeake Bay nitrogen fluxes derived from a land-estuarine ocean biogeochemical modeling system: Model description, evaluation, and nitrogen budgets. *Journal of Geophysical Research: Biogeosciences*, *120*, 1666–1695. https://doi.org/10.1002/2015JG002931

Filippino, K. C., Bernhardt, P. W., & Mulholland, M. R. (2009). Chesapeake Bay plume morphology and the effects on nutrient dynamics and primary productivity in the coastal zone. *Estuaries and Coasts*, *32*(3), 410–424. https://doi.org/10.1007/s12237-009-9139-y

Fisher, D. C., & Oppenheimer, M. (1991). Atmospheric nitrogen deposition and the Chesapeake Bay estuary. *Ambio*, *20*(3/4), 102–108. http://www.jstor.org/stable/4313793

Fisher, T., Gustafson, A., Sellner, K., Lacouture, R., Haas, L. W., Wetzel, R. L., et al. (1999). Spatial and temporal variation of resource limitation in Chesapeake Bay. *Marine Biology*, *133*(4), 763–778. https://doi.org/10.1007/s002270050518

Fisher, T. R., Hagy, J. D., & Rochelle-Newall, E. (1998). Dissolved and particulate organic carbon in Chesapeake Bay. *Estuaries*, *21*(2), 215–229. https://doi.org/10.2307/1352470

Gantt, B., Kelly, J. T., & Bash, J. (2015). Updating sea spray aerosol emissions in the Community Multiscale Air Quality (CMAQ) model version 5.0.2. *Geoscientific Model Development*, *8*, 3733–3746. https://doi.org/10.5194/gmd-8-3733-2015

Geyer, W. R. (2010). Estuarine salinity structure and circulation. In A. Valle-Levinson (Ed.), *Contemporary issues in estuarine physics* (pp. 12–26). Cambridge, UK: Cambridge University. https://doi.org/10.1017/CBO9780511676567.003

Grimm, J. (2017). Extension of ammonium and nitrate wet-fall deposition models for the Chesapeake Bay watershed. The Pennsylvania State University. (ftp://ftp. chesapeakebay.net/modeling/Phase6/Draft_Phase_6/Documentation/03H%20Final_Report_Extension_of_Ammonium_and_Nitrate_Wet-Fall_Deposition_Models_for_the_CBW_Jan2017.pdf)

Grimm, J., & Lynch, J. (2005). Improved daily precipitation nitrate and ammonium concentration models for the Chesapeake Bay watershed. *Environmental Pollution*, *135*(3), 445–455. https://doi.org/10.1016/j.envpol.2004.11.018

Hagy, J. D., Boynton, W. R., & Jasinski, D. A. (2005). Modelling phytoplankton deposition to Chesapeake Bay sediments during winter-spring: Interannual variability in relation to river flow. *Estuarine, Coastal and Shelf Science*, *62*(1–2), 25–40. https://doi.org/10.1016/j.ecss.2004.08.004

Hagy, J. D., Boynton, W. R., Keefe, C. W., & Wood, K. V. (2004). Hypoxia in Chesapeake Bay, 1950–2001: Long-term change in relation to nutrient loading and river flow. *Estuaries*, *27*(4), 634–658. https://doi.org/10.1007/BF02907650

Harding, L. W., Gallegos, C., Perry, E., Miller, W., Adolf, J., Mallonee, M., & Paerl, H. W. (2016). Long-term trends of nutrients and phytoplankton in Chesapeake Bay. *Estuaries and Coasts*, *39*(3), 664–681. https://doi.org/10.1007/s12237-015-0023-7

Harding, L. W., Mallonee, M. E., & Perry, E. S. (2002). Toward a predictive understanding of primary productivity in a temperate, partially stratified estuary. *Estuarine, Coastal and Shelf Science*, *55*(3), 437–463. https://doi.org/10.1006/ecss.2001.0917

Hickey, B. M., & Banas, N. S. (2003). Oceanography of the US Pacific Northwest coastal ocean and estuaries with application to coastal ecology. *Estuaries*, *26*(4), 1010–1031. https://doi.org/10.1007/BF02803360

Hinga, K. R., Keller, A. A., & Oviatt, C. A. (1991). Atmospheric deposition and nitrogen inputs to coastal waters. *Ambio*, *20*(6), 256–260. http://www.jstor.org/stable/4313835

Hofmann, E., Druon, J., Fennel, K., Friedrichs, M. A. M., Haidvogel, D., Lee, C., et al. (2008). Eastern US continental shelf carbon budget integrating models, data assimilation, and analysis. *Oceanography*, *21*(1), 86–104. https://doi.org/10.5670/oceanog.2008.70

Holland, A., Shaughnessy, A. T., & Hiegel, M. H. (1987). Long-term variation in mesohaline Chesapeake Bay macrobenthos: Spatial and temporal patterns. *Estuaries*, *10*(3), 227–245. https://doi.org/10.2307/1351851

Irby, I. D. (2017). Using water quality models in management—A multiple model assessment, analysis of confidence, and evaluation of climate change impacts. Dissertations, theses, and masters projects. Paper 1516639464. https://doi.org/10.21220/V5P15T

Irby, I. D., Friedrichs, M. A. M., Da, F., & Hinson, K. E. (2018). The competing impacts of climate change and nutrient reductions on dissolved oxygen in Chesapeake Bay. *Biogeosciences*, *15*(9), 2649–2668. https://doi.org/10.5194/bg-15-2649-2018

Irby, I. D., Friedrichs, M. A. M., Friedrichs, C. T., Bever, A. J., Hood, R. R., Lanerolle, L. W., & Scully, M. E. (2016). Challenges associated with modeling low-oxygen waters in Chesapeake Bay: A multiple model comparison. *Biogeosciences*, *13*(7), 2011–2028. https://doi.org/10.5194/bg-13-2011-2016

Janowitz, G. S., & Pietrafesa, L. J. (1982). The effects of alongshore variation in bottom topography on a boundary current—(topographically induced upwelling). *Continental Shelf Research*, *1*(2), 123–141. https://doi.org/10.1016/0278-4343(82)90001-2

Jerlov, N. G. (1976). *Marine optics*, *Elsevier Oceanography Series* (Vol. 14). Amsterdam, Netherlands: Elsevier.

Jiang, L., & Xia, M. (2018). Modeling investigation of the nutrient and phytoplankton variability in the Chesapeake Bay outflow plume. *Progress in Oceanography*, *162*, 290–302. https://doi.org/10.1016/j.pocean.2018.03.004

Jolliff, J. K., Kindle, J. C., Shulman, I., Penta, B., Friedrichs, M. A. M., Helber, R., & Arnone, R. A. (2009). Summary diagrams for coupled hydrodynamic-ecosystem model skill assessment. *Journal of Marine Systems*, *76*(1–2), 64–82. https://doi.org/10.1016/j.jmarsys.2008.05.014

Keene, W., Montag, J., Maben, J., Southwell, M., Leonard, J., Church, T., et al. (2002). Organic nitrogen in precipitation over eastern North America. *Atmospheric Environment*, *36*(28), 4529–4540. https://doi.org/10.1016/S1352-2310(02)00403-X

Kemp, W. M., Boynton, W. R., Adolf, J. E., Boesch, D. F., Boicourt, W. C., Brush, G., et al. (2005). Eutrophication of Chesapeake Bay: Historical trends and ecological interactions. *Marine Ecology Progress Series*, *303*, 1–29. https://doi.org/10.3354/meps303001

Kemp, W. M., Smith, E. M., Marvin-DiPasquale, M. M., & Boynton, W. R. (1997). Organic carbon balance and net ecosystem metabolism in Chesapeake Bay. *Marine Ecology Progress Series*, *150*, 229–248. https://doi.org/10.3354/meps150229

Kremer, J. N., & Nixon, S. W. (1978). *A coastal marine ecosystem, simulation and analysis*. New York: Springer-Verlag. https://doi.org/10.1007/978-3-642-66717-6

Li, M., Lee, Y. J., Testa, J. M., Li, Y., Ni, W., Kemp, W. M., & Di Toro, D. M. (2016). What drives interannual variability of hypoxia in Chesapeake Bay: Climate forcing versus nutrient loading? *Geophysical Research Letters*, *43*, 2127–2134. https://doi.org/10.1002/2015GL067334

Li, Y., Schichtel, B. A., Walker, J. T., Schwede, D. B., Chen, X., Lehmann, C. M., et al. (2016). Increasing importance of deposition of reduced nitrogen in the United States. *Proceedings of the National Academy of Sciences of the United States of America*, *113*(21), 5874–5879. https://doi.org/10.1073/pnas.1525736113

Linker, L. C., Dennis, R., Shenk, G. W., Batiuk, R. A., Grimm, J., & Wang, P. (2013). Computing atmospheric nutrient loads to the Chesapeake Bay watershed and tidal waters. *JAWRA Journal of the American Water Resources Association*, *49*(5), 1025–1041. https://doi.org/10.1111/jawr.12112

Lomas, M. W., Gilbert, P. M., Shiah, F. K., & Smith, E. M. (2002). Microbial processes and temperature in Chesapeake Bay: Current relationships and potential impacts of regional warming. *Global Change Biology*, *8*(1), 51–70. https://doi.org/10.1046/j.1365-2486.2002.00454.x

Mannino, A., Signorini, S. R., Novak, M. G., Wilkin, J., Friedrichs, M. A. M., & Najjar, R. G. (2016). Dissolved organic carbon fluxes in the Middle Atlantic Bight: An integrated approach based on satellite data and ocean model products. *Journal of Geophysical Research: Biogeosciences*, *121*, 312–336. https://doi.org/10.1002/2015JG003031

Marchesiello, P., McWilliams, J., & Shchepetkin, A. (2001). Open boundary conditions for long-term integration of regional oceanic models. *Ocean Modelling*, *3*(1-2), 1–20. https://doi.org/10.1016/S1463-5003(00)00013-5

Melrose, D.C., Rebuck, N.D., Townsend, D. W., Thomas, M., & Taylor, C. (2015). Ammonia, silicate, phosphate, nitrite + nitrate, dissolved oxygen, and other variables collected from profile and discrete sample observations using CTD, nutrient autoanalyzer, and other instruments from NOAA Ship Delaware II, NOAA Ship Gordon Gunter, NOAA Ship Henry B. Bigelow, NOAA Ship Okeanos Explorer, and NOAA Ship Pisces in the Gulf of Maine, Georges Bank, and Mid-Atlantic Bight from 2009-11-03 to 2016-08-19 (NCEI Accession 0127524). Version 9.9. NOAA National Centers for Environmental Information. Dataset. https://doi.org/10.7289/V5HQ3WV3

Mesinger, F., DiMego, G., Kalnay, E., Mitchell, K., Shafran, P. C., Ebisuzaki, W., et al. (2006). North American regional reanalysis. *Bulletin of the American Meteorological Society*, *87*(3), 343–360. https://doi.org/10.1175/BAMS-87-3-343

Moriarty, J. M., Harris, C. K., Fennel, K., Friedrichs, M. A. M., Xu, K., & Rabouille, C. (2017). The roles of resuspension, diffusion and biogeochemical processes on oxygen dynamics offshore of the Rhône River, France: A numerical modeling study. *Biogeosciences*, *14*, 1919–1946. https://doi.org/10.5194/bg-14-1919-2017

Murphy, R. R., Kemp, W. M., & Ball, W. P. (2011). Long-term trends in Chesapeake Bay seasonal hypoxia, stratification, and nutrient loading. *Estuaries and Coasts*, *34*(6), 1293–1309. https://doi.org/10.1007/s12237-011-9413-7

Najjar, R. G., Herrmann, M., Aleander, R., Boyer, E. W., Burdige, D., Butman, D., et al. (2018). Carbon budget of tidal wetlands, estuaries, and shelf waters of eastern North America. *Global Biogeochemical Cycles*, *32*, 389–416. https://doi.org/10.1002/2017GB005790

Newcombe, C. L., & Horne, W. A. (1938). Oxygen-poor waters of the Chesapeake Bay. *Science*, *88*(2273), 80–81. https://doi.org/10.1126/science.88.2273.80

Nixon, S. W. (1995). Coastal marine eutrophication: A definition, social causes, and future concerns. *Ophelia*, *41*(1), 199–219. https://doi.org/10.1080/00785236.1995.10422044

Paerl, H. W., Dennis, R. L., & Whitall, D. R. (2002). Atmospheric deposition of nitrogen: Implications for nutrient over-enrichment of coastal waters. *Estuaries*, *25*(4), 677–693. https://doi.org/10.1007/BF02804899

Paerl, H. W., Willey, J. D., Go, M., Peierls, B. L., Pinckney, J. L., & Fogel, M. L. (1999). Rainfall stimulation of primary production in western Atlantic Ocean waters: Roles of different nitrogen sources and co-limiting nutrients. *Marine Ecology Progress Series*, *76*, 205–214.

Paerl, H. W. (1997). Coastal eutrophication and harmful algal blooms: Importance of atmospheric deposition and groundwater as "new" nitrogen and other nutrient sources. *Limnology and Oceanography*, *42*, 1154–1165. https://doi.org/10.4319/lo.1997.42.5_part_2.1154

Paulson, C. A., & Simpson, J. J. (1977). Irradiance measurements in the upper ocean. *Journal of Physical Oceanography*, *7*, 952–956. https://doi.org/10.1175/1520-0485(1977)007<0952:IMITUO>2.0.CO;2

Pietrafesa, L., Morrison, J. M., McCann, M., Churchill, J., Böhm, E., & Houghton, R. (1994). Water mass linkages between the Middle and South Atlantic Bights. *Deep Sea Research Part II: Topical Studies in Oceanography*, *41*(2), 365–389. https://doi.org/10.1016/0967-0645(94)90028-0

Prospero, J., Barrett, K., Church, T., Dentener, F., Duce, R., Galloway, J., et al. (1996). Atmospheric deposition of nutrients to the North Atlantic Basin. *Biogeochemistry*, *35*(1), 27–73. https://doi.org/10.1007/BF02179824

Russell, K. M., Galloway, J. N., Macko, S. A., Moody, J. L., & Scudlark, J. R. (1998). Sources of nitrogen in wet deposition to the Chesapeake Bay region. *Atmospheric Environment*, *32*(14), 2453–2465. https://doi.org/10.1016/S1352-2310(98)00044-2

Sarwar, G., Godowitch, J., Henderson, B., Fahey, K., Pouliot, G., Hutzell, B., et al. (2013). A comparison of atmospheric composition using the carbon bond and regional atmospheric chemistry mechanisms. *Atmospheric Chemistry and Physics*, *13*(19), 9675–9712.

Schwede, D. B., & Lear, G. G. (2014). A novel hybrid approach for estimating total deposition in the United States. *Atmospheric Environment*, *92*, 207–220. https://doi.org/10.1016/j.atmosenv.2014.04.008

Scully, M. E. (2013). Physical controls on hypoxia in Chesapeake Bay: A numerical modeling study. *Journal of Geophysical Research: Oceans*, *118*, 1239–1256. https://doi.org/10.1002/jgrc.20138

Scully, M. E. (2016). Mixing of dissolved oxygen in Chesapeake Bay driven by the interaction between wind-driven circulation and estuarine bathymetry. *Journal of Geophysical Research: Oceans*, *121*, 5639–5654. https://doi.org/10.1002/2016JC011924

Seliger, H. H., Boggs, J. A., & Biggley, W. H. (1985). Catastrophic anoxia in the Chesapeake Bay in 1984. *Science*, *228*(4695). https://doi.org/10.1126/science.228.4695.70

Shchepetkin, A., & McWilliams, J. (2005). The regional ocean modeling system (ROMS): A split-explicit, free-surface, topography-following-coordinate ocean model. *Ocean Model*, *9*, 347–404. https://doi.org/10.1016/j.ocemod.2004.08.002

Shenk, G. W., & Linker, L. C. (2013). Development and application of the 2010 Chesapeake Bay watershed total maximum daily load model. *JAWRA Journal of the American Water Resources Association*, *49*(5), 1042–1056. https://doi.org/10.1111/jawr.12109

Shiah, F. K., & Ducklow, H. W. (1994). Temperature regulation of heterotrophic bacterioplankton abundance, production, and specific growth rate in Chesapeake Bay. *Limnology and Oceanography*, *39*, 1243–1258. https://doi.org/10.4319/lo.1994.39.6.1243

Skamarock, W. C., Klemp, J. B., Dudhia, J., Gill, D. O., Barker, D. M., Dudha, M. G., et al. (2008). A description of the Advanced Research WRF version 30, NCAR technical note, Technical Report, NCAR/TN-475.

Smolarkiewicz, P. K. (1983). A simple positive definite advection scheme with small implicit diffusion. *Monthly Weather Review*, *111*(3), 479–486. https://doi.org/10.1175/1520-0493(1983)111<0479:ASPDAS>2.0.CO;2

Smolarkiewicz, P. K. (1984). A fully multidimensional positive definite advection transport algorithm with small implicit diffusion. *Journal of Computational Physics*, *54*(2), 325–362. https://doi.org/10.1016/0021-9991(84)90121-9

Son, S., Wang, M., & Harding, L. W. (2014). Satellite-measured net primary production in the Chesapeake Bay. *Remote Sensing of Environment*, *144*, 109–119. https://doi.org/10.1016/j.rse.2014.01.018

St-Laurent, P., Friedrichs, M. A. M., Najjar, R. G., Martins, D. K., Herrmann, M., Miller, S. K., & Wilkin, J. (2017). Impacts of atmospheric nitrogen deposition on surface waters of the western North Atlantic mitigated by multiple feedbacks. *Journal of Geophysical Research: Oceans*, *122*, 8406–8426. https://doi.org/10.1002/2017JC013072

Testa, J. M., & Kemp, W. M. (2014). Spatial and temporal patterns of winter-spring oxygen depletion in Chesapeake Bay bottom water. *Estuaries and Coasts*, *37*(6), 1432–1448. https://doi.org/10.1007/s12237-014-9775-8

Tian, H., Yang, Q., Najjar, R. G., Ren, W., Friedrichs, M. A. M., Hopkinson, C. S., & Pan, S. (2015). Anthropogenic and climatic influences on carbon fluxes from eastern North America to the Atlantic Ocean: A process-based modeling study. *Journal of Geophysical Research: Biogeosciences*, *120*, 752–772. https://doi.org/10.1002/2014JG002760

Townsend, D. W., Thomas, A. C., Mayer, L. M., Thomas, M. A., & Quinlan, J. A. (2006). Oceanography of the Northwest Atlantic continental shelf. In A. R. Robinson, & K. H. Brink (Eds.), *The Sea* (Vol. 14A, pp. 119–168). Cambridge, MA: Harvard University Press.

USEPA (U.S. Environmental Protection Agency) (2010a). Chesapeake Bay total maximum daily load for nitrogen, phosphorus and sediment appendix L: Setting the Chesapeake Bay atmospheric nitrogen deposition allocations. U.S. Environmental Protection Agency, Chesapeake Bay Program Office, Annapolis, Maryland. http://www.epa.gov/reg3wapd/pdf/pdf_chesbay/FinalBayTMDL/AppendixLAtmosNDepositionAllocations_final.pdf

USEPA (U.S. Environmental Protection Agency) (2010b). Chesapeake Bay phase 5.3 community watershed model: Section 1. Phase 5.3 Watershed model overview. U.S. Environmental Protection Agency, Chesapeake Bay Program Office, Annapolis, Maryland. ftp://ftp.chesapeakebay.net/modeling/P5Documentation/SECTION_1.pdf

USEPA (U.S. Environmental Protection Agency) (2010c). Chesapeake Bay phase 5.3 community watershed model: Section 11. Simulation and calibration of riverine fate and transport of nutrients and sediment. U.S. Environmental Protection Agency, Chesapeake Bay Program Office, Annapolis, Maryland. ftp://ftp.chesapeakebay.net/Modeling/P5Documentation/SECTION_11.pdf

Williams, R. G., McDonagh, E., Roussenov, V. M., Torres-Valdes, S., King, B., Sanders, R., & Hansell, D. A. (2011). Nutrient streams in the North Atlantic: Advective pathways of inorganic and dissolved organic nutrients. *Global Biogeochemical Cycles*, *25*, GB4008. https://doi.org/10.1029/2010GB003853

Xiao, Y., & Friedrichs, M. A. M. (2014a). Using biogeochemical data assimilation to assess the relative skill of multiple ecosystem models: Effects of increasing the complexity of the planktonic food web. *Biogeosciences*, *11*(11), 3015–3030. https://doi.org/10.5194/bg-11-3015-2014

Xiao, Y., & Friedrichs, M. A. M. (2014b). The assimilation of satellite-derived data into a one-dimensional lower trophic level marine ecosystem model. *Journal of Geophysical Research: Oceans*, *119*, 2691–2712. https://doi.org/10.1002/2013JC009433

Xu, J., Long, W., Wiggert, J. D., Lanerolle, L. W. J., Brown, C. W., Murtugudde, R., & Hood, R. R. (2012). Climate forcing and salinity variability in Chesapeake Bay, USA. *Estuarine, Coastal and Shelf Science*, *35*(1), 237–261. https://doi.org/10.1007/s12237-011-9423-5